MULTIOMICS AND DIGITAL MONITORING DURING LIFESTYLE CHANGES REVEAL INDEPENDENT DIMENSIONS OF HUMAN BIOLOGY AND HEALTH

Francesco Marabita[1,2], Tojo James[1,2], Anu Karhu[1], Robert Mills[1], Teemu Perheentupa[1], Hans Stenlund[3], Fredrik Boulund[4], Cecilia Hellström[5], Maja Neiman[5], Heidi Virtanen[1], Kaisa Kettunen[6,1], Hannele Laivuori[1,7,8] Pyry Helkkula[1], Myles Byrne[1], Harri Honko[9], Antti Kallonen[9], Miikka Ermes[10], Heidi Similä[10], Mikko Lindholm[10], Elisabeth Widen[1], Samuli Ripatti[1], Maritta Perälä-Heape[11,12], Lars Engstrand[4], Peter Nilsson[5], Thomas Moritz[3,13], Timo Miettinen[1], Riitta Sallinen[1,2], Olli Kallioniemi[1,2]

[1]Institute for Molecular Medicine Finland (FIMM), HiLIFE, University of Helsinki, Helsinki, Finland. [2]Science for Life Laboratory, Department of Oncology-Pathology, Karolinska Institutet, Stockholm, Sweden. [3]Science for Life Laboratory, Swedish Metabolomics Centre, Department of Forest Genetics and Plant Physiology, Swedish University of Agricultural Sciences, Umeå, Sweden. [4]Science for Life Laboratory, Center for Translational Microbiome Research, Department of Microbiology, Tumor and Cell biology, Karolinska Institutet, Stockholm, Sweden. [5]Science for Life Laboratory, Division of Affinity Proteomics, Department of Protein Science, KTH Royal Institute of Technology, Stockholm, Sweden. [6]HUS Diagnostic Center, Laboratory of Genetics, University of Helsinki and Helsinki University Hospital, Helsinki, Finland. [7]Medical and Clinical Genetics, University of Helsinki and Helsinki University Hospital, Helsinki, Finland. [8]Department of Obstetrics and Gynecology, Tampere University Hospital and Tampere University, Faculty of Medicine and Health Technology, Tampere, Finland. [9]Tampere University of Technology, Tampere, Finland [10]VTT Technical Research Centre of Finland, Espoo, Finland. [11]Faculty of Medicine, University of Oulu, Oulu, Finland. [12]Centre for Health and Technology, University of Oulu, Oulu, Finland. [13]Novo Nordisk Foundation Center for Basic Metabolic Research, Faculty of Health and Medical Sciences, University of Copenhagen, Copenhagen, Denmark.

ABSTRACT

We collected clinical measurements, health surveys and multiomics profiles (genomics, proteomics, autoantibodies, metabolomics and gut microbiome) from 96 individuals over 16 months, along with daily activity and sleep monitoring. Between- and within-individual variability was analysed as the participants underwent data-driven health coaching. Multiomics factor analysis resulted in an unsupervised integrated view of the data, with individual factors explaining distinct aspects of variability in human health and lifestyle, such as obesity, diabetes, liver function, cardiovascular disease, inflammation, immunity, hormonal function, exercise and diet. The data revealed both known and new associations between molecular pathways, risk factors, behaviour and lifestyle aspects. Data-driven analysis of multidimensional molecular and digital signatures of participants over time enabled deep understanding of biological variability between people as well as the systemic effects of lifestyle changes. Our study facilitates a detailed evaluation of aspects impacting on health and underlines the importance of personal molecular signatures.

Monitoring of human health, impact of lifestyle and disease development is possible by longitudinal measurements of clinical laboratory tests, omics technologies, or digital health monitoring using wearable sensors. This provides opportunities to explore human systems biology and to predict and intervene in processes leading to disease development. However, our knowledge and ability to make use of such data and define actionable insights, correlations and causal patterns are limited. There is a lack of deep integrated datasets, where different dimensions of human biology have been explored at the same time. Each individual has a unique profile, composed of genetic, epigenetic, molecular, clinical and lifestyle parameters, which may change over time during development, aging and disease transitions. These processes cannot be understood as a single general pathway for the average human or patient, but they can best be described as a collection of individual trajectories. Several studies have investigated the use of individualized molecular profiles to assess disease risks or the connection between omics measurements and clinical tests, using an n-of-one longitudinal approach[1,2], a cross-sectional design [3], a controlled longitudinal perturbation study [4], or a cohort study with personal behavioural coaching[5]. More recently, other studies[6-8] analysed longitudinal data over an extended time period in a cohort of individuals at risk for diabetes, while another prospective observational study investigated the stability of the individual molecular signatures[9].

The Digital Health Revolution (DHR) program[10] in 2015-2020 was based on the concept that future healthcare strategies will evolve in a direction which allows citizens to control and make use of their own personal data to improve their health and wellness. The project aimed at implementing proactive P4 (predictive, preventive, personalized, and participatory) healthcare with multi-level molecular and digital data. Within this framework, we integrated deep multi-omics profiles and connected them to health surveys, clinical observations and digital health measurements. We aimed to: 1) integrate longitudinal multi-omics data between and within people over time; 2) exploit the discovered associations to understand novel links between molecular and clinical data; and 3) verify if data feedback and coaching would guide and motivate people to make lifestyle changes. Overall, we aimed at achieving a holistic understanding of the variables involved in different aspects of human biology and health. To accomplish these goals, we applied multi-omics factor analysis and connected the learned factors with interpretable features of health and behaviour.

RESULTS

STUDY OVERVIEW

We carried out a 16-month longitudinal study on 96 individuals (aged 25-59) recruited from an occupational healthcare clinic in Helsinki, Finland (Supplementary Figure 1-2 and Supplementary Table 1). The participants had no previously diagnosed serious chronic diseases, although we allowed individuals with risk factors for chronic diseases. We acquired comprehensive measurements of health and behaviour, including anthropometrics, clinical laboratory tests, questionnaire data, physical fitness tests and activity and sleep quantification with a wearable device. In addition, we performed a series of omics measurements to study the genome, the plasma proteome and metabolome, the autoantibody profile and the gut microbiome. The prospective collection of molecular and digital profiles resulted in a thorough longitudinal dataset of human health and lifestyle aspects (Figure 1). This allowed to define baseline molecular profiles and longitudinal trajectories of health data in the participants during a personalized lifestyle coaching. We collected over 20,000 biological samples during five study visits and generated a compendium of >53 million primary data points, for 558,032 distinct features. Two types of feedback were applied to stimulate and motivate lifestyle changes. First, actionable health data were returned to participants through a web dashboard and interpreted by a study physician, starting from the second visit. Second, personal data-driven coaching was provided, including three face-to-face and six remote meetings, plus continuous email and phone support, starting from the third visit. Personal actionable possibilities were identified with the help of questionnaires, clinical laboratory tests and physical examination, and focused on diet, exercise, mental wellbeing, stress and time management. Of the 107 people enrolled, 96 completed the study. The data-driven coaching positively impacted on the health of the participants, and 86% reported subjective improvement in at least of the following aspects: diet, exercise, sleep, mental wellbeing, stress management, drinking or smoking (Supplementary Figure 3). For example, the percentage of people who did not exercise decreased from 9% to 1%, the percentage of smokers decreased from 16% to 8%, and the percentage of daily drinkers from 8% to 5%. The participants felt that the wearable device, return of personal health data, and tailored coaching were the most motivating aspects of the

study. Overall, the subjects were enthusiastic about participating and 76% indicated that they would again take part in a similar study.

LONGITUDINAL ACTIONABLE CHANGES

We defined a *phenotype* using the ensemble of questionnaires, anthropometrics, vitals and clinical laboratory tests. Actionable health issues were defined at baseline, including dyslipidaemia, overweight and obesity, elevated systolic blood pressure, low vitamin D, elevated blood glucose, anaemia and self-reported obstructive sleep apnea (Supplementary table 1 and Supplementary Figure 4).

We first analysed the clinical measurements at baseline to define the group of individuals with Out-Of-Range (OORB) values. To explore if the data feedback and coaching had a positive effect on objective health parameters, we modelled the longitudinal changes in the ORRB individuals, based on the assumption that measurements outside the reference values represented an actionable finding to improve lifestyle and health. We analysed the average change per visit, adjusting for sex and age. We found significant improvements (FDR<0.05) in several key health parameters for the OORB group during the course of the study, such as an increase in vitamin D levels and a decrease in blood pressure, LDL-cholesterol, and total/HDL cholesterol ratio (Figure 2 and Supplementary Table 3).

Secondly, we obtained an overview of all the clinical variables and compared the individuals using Principal Component Analysis (PCA). The first three PCs (Figure 2) accounted for 44.8% of the variance and the major drivers of variability were cardiometabolic variables (for PC1 and PC3: BMI, insulin, fasting glucose, cholesterol, and lipoprotein profiles) and sex-dependent anthropometrics and hematological measurements (PC2). Trajectories for selected individuals showed the changes during the multiple study visits and visualized the improvements in the clinical parameters (Figure 2 and Supplementary Figure 5).

118 In summary, we showed that the return of data as well as data-driven lifestyle coaching resulted in objective improvements of health behaviour and health outcomes, including physiological and
120 laboratory measurements indicative of cardiovascular risk.

MULTIOMICS SIGNATURES

122 *DISTINCT SOURCES OF MOLECULAR VARIABILITY*

We next generated multiomics profiles and set out to explore the association of these variables with
124 each other and with the clinical features. We first investigated the sources of variability in the omics, by partitioning the variance for each feature into personal variation (i.e. between-individual), known
126 factors (age, sex and study visit) and residual unknown sources (for example biological, environmental or technical aspects). We found that the personal variation impacted all data types but to a different
128 extent (Supplementary Figure 6). Autoantibodies represented a highly personal signature and on average 92% of the variance was explained by personal variation. Metabolites were dominated by
130 personal variation (56-71% on average) but residual components were also present (23-35% on average). Proteins had similar average personal (49%) and residual components (45%). The
132 microbiome data was dominated by unexplained factors (68% on average). These results were confirmed by an alternative distance-based method (Supplementary Figure 6). We observed that the
134 average within-individual distance was lower than the between-individual distance, to a different extent for different omics, and autoantibodies showed the lowest within-individual distance, i.e. high
136 similarity.

UNDERSTANDING THE MOLECULAR VARIABILITY

138 We used Multi-Omics Factor Analysis (MOFA+)[11,12] to carry out an unsupervised analysis of the complete multiomics data, hence excluding the clinical variables and other phenotypic data. MOFA+
140 helped to integrate and interpret the measurements and their variability across all the omics layers. MOFA+ resulted in an interpretable low-dimensional representation in the form of a small number of
142 independent factors that captured the major sources variability in the data and originated from simultaneous inclusion of baseline and longitudinal differences. The analysis facilitated the
144 identification of subgroups of samples and the molecular features that contributed to the ordination of

the samples in the dimensions defined by the factors. An overview of the samples based on the learned factors is given in Supplementary Figure 7. We identified 14 factors (F1-F14), each explaining a minimum of 2% of the variance in at least one data type. The fraction of the total variance explained across the six omics types varied from 6% for gut microbiome to 95% for the autoantibodies (Figure 3). The learned factors were either predominantly associated with one omics type or contributed to several omics types, suggesting that the underlying biological determinants might affect different types of measurements simultaneously. We then explored the molecular basis of each factor. First, we investigated the contribution of the original omics features, by inspecting the loadings on each factor, which represent their weights, in order to interpret the nature of the associated biological domains. Second, we tested the association between the factors and the phenotype, including questionnaire data, clinical variables, fitness tests, activity and sleep data, and other metrics. Each factor was linked to specific phenotypic characteristics (linear models, FDR<0.001, Figure 3 and Supplementary Table 4). Importantly, most of the factors were associated with distinct sets of variables across the different categories and thereby defined molecular patterns that were linked to distinct aspects of lifestyle and health, including modifiable behavioural aspects, such as diet and exercise. We then refined the top associations for each factor with a covariate-adjusted statistical model. We aimed at accounting for the correlation among observations from the same individual and fitted a linear mixed model (LMM), with age and sex as fixed effects and the individual as a random effect. We also interpreted the association in view of the contributing molecular features and pathways and the results are presented below.

Obesity and insulin resistance. The top features with high positive loadings on F11 included plasma proteins involved in pathways known to be dysregulated in obesity or dyslipidemia (LEP[13], IL-1ra (IL1RN)[14], t-PA (PLAT)[15], FABP4[16], FGF21[17], IL-6[14], LDL receptor[18]). Interestingly, several proteins reported as protective factors against obesity (GH1, IGFBP1, PON3)[19-21] had negative loadings. We found significant correlations between F11 and well-known metabolic traits and clinical measurements (Figure 4 and Supplementary figure 9). These included positive association with BMI (p_{lmm}=1.53E−21), LDL-cholesterol levels (p_{lmm}=4.47E−03) and insulin resistance ($\log_{10}$HOMA-IR, p_{lmm}=6.51E−14). Also,

172 we found a negative association with HDL-cholesterol (p_{lmm} =2.16E-06) as well as with measures of physical activity and fitness gathered from the questionnaire, such as leisure-time exercise 174 (p_{lmm}=1.06E−03) and exercise habits (p_{lmm}=8.25E−04), or the activity levels in terms of steps/day measured by the wearable device (p_{lmm}=0.01). An inverse correlation was also observed with physical 176 fitness at the level of upper body (p_{lmm}=5.53E−05) abdominal (p_{lmm}=1.59E−03) and lower body (p_{lmm}=1.14E−03). Participants with first-degree relatives with diabetes had higher factor values 178 compared to the individuals who did not report family-history for diabetes (p_{lmm}=6.25E−03). Finally, an individual who was diagnosed with type 2 diabetes during the study had the highest factor values. We 180 therefore interpreted F11 as strongly related to obesity, insulin resistance and diabetes risk and pathogenesis as well as clearly associated with quantitative data on exercise and mobility. F11 was 182 also associated with overall health, as evidenced by a negative association with self-reported overall health (p_{lmm}=9.26E−07) and a positive correlation with predicted coronary heart disease (CHD) risk 184 (p_{lmm}=0.01). In summary, F11 assisted in estimating molecular patterns of health and behaviour that are associated with obesity as well as potential trajectories leading to diabetes.

186 **Impact of hormones and ethinyl estradiol.** F9 was influenced by sex and sex-specific biological differences in multiomics. In contrast, F14 was linked to the use hormone replacement therapy or 188 hormonal contraception in women. Particularly, young women reporting the use of a contraceptive containing ethinyl estradiol (EE) had elevated F14 values (p_{lmm}=2.28e−10). F14 appeared to be almost 190 exclusively linked to the use of EE. Consistent with this observation, known estrogen-sensitive proteins had the highest positive weights for F14 (Figure 4), but there were also contributions from cortisol and 192 thyroxine levels, which we interpreted as potential secondary effects[22,23]. Pulse (p_{lmm}=9.32E−03), hsCRP (log-transformed, p_{lmm}=7.40E−09) and leukocyte numbers (log-transformed, p_{lmm}=6.09e−05) 194 also positively correlated with F14 and alterations of these clinical laboratory parameters were prominent in women with particularly high factor values. These observations indicated that EE use is 196 associated with strong and distinct effects on human biology, which may lead to increased levels of inflammation, impact on thyroid and cortisol levels as well as physiological effects.

198 **Dietary habits.** F3 and F6 were mostly connected to the metabolome, they were associated with dietary habits (Supplementary figure 10), such as reported consumption of fresh fruit and vegetables.
200 However, all the predictors were not significantly associated to the factors (p_{lmm}>0.05) in the covariate-adjusted models, suggesting that the association may be explained by individual-specific (person-to-
202 person) differences and not by changes of the diet during the study. Moreover, caffeine and its metabolites were abundantly represented among the features with largest loadings for F7 (Figure 4),
204 and indeed this factor was strongly correlated with self-reported coffee consumption (p_{lmm}=7.63E−12).

Lipids, free fatty acids and fatty acid esters. F5, F8 and F12 (Supplementary figure 11) were each
206 associated with distinct aspects of plasma lipid composition. In particular, free fatty acids (FFA) contributed mostly to F12, while fatty acid esters (FAEs), mostly in the form of acylcarnitines,
208 contributed to F5 and F8. In the postabsorptive state, blood FFA are a result of lipolysis from adipose tissue and they reflect dietary intake[24], while changes in the acylcarnitine pool can be linked to changes
210 in fatty acid oxidation. Accumulation of acylcarnitines as products of incomplete mitochondrial fatty acid oxidation has been associated with obesity and diabetes[25]. Even after adjusting for the covariates,
212 F12 was negatively associated with blood pressure (systolic, p=0.035; diastolic p=0.021), in line with the known association between FFA and hypertension[26]. F5 and F8 were both strongly associated with
214 clinical measurements indicating dyslipidemia, including total cholesterol (p_{lmm}=1.64E-08 and p_{lmm}=8.48E−10) LDL cholesterol (p_{lmm}=7.13E-06 and p_{lmm}=1.74E−05), triglycerides (p_{lmm}=3.74E-05 and
216 p_{lmm}=8.45E−7) and ApoB (p_{lmm}=3.24E-08 and p_{lmm}=9.11E−06), thus implicating dysregulation of lipid metabolism as an underlying influence for F5 and F8. Importantly, they were only weakly associated
218 with BMI (R2=0.004 and R2=0.006; p_{lmm}=0.05 and p_{lmm}=0.07), suggesting that these two factors were associated with dyslipidemia independently of obesity. Sex was a significant covariate for the
220 associations seen for F5 (maximum p_{lmm}=1.21E-05) but not for F8 (minimum p_{lmm}=0.73).

Hepatic function. Metabolites connected to liver function had major loadings on F2 (Supplementary
222 figure 12). Bile acids or their glycine or taurine conjugates had negative weights and a major impact in the classification of the individuals along the F2 axis. The involvement of the liver function in
224 determining F2 values was supported by the contribution of other liver-associated metabolites that on

average were increased in the samples with negative factor values. These metabolites are known to
226 be increased in blood after liver disease (biliverdin) or used to eliminate the hepatic nitrogen pool (glutamine, hippuric acid, phenylacetylglutamine). The liver is a fundamental organ in maintaining
228 metabolic homeostasis, it modulates the composition of the blood metabolome and therefore we assumed that F2 reflected the structural and functional integrity of the liver.

230 **Autoantibodies.** F1 was mostly explained by the presence of autoantibodies, which did not contribute importantly to other factors. F1 was influenced by the binary nature of the autoantibody data
232 (presence/absence) and due to the stable autoantibody signature over time. Indeed, autoantibodies can be considered as an IgG reactivity barcode for each individual[27]. F1 correlated well with the
234 autoantibody counts and to a lesser extent with the age (Supplementary Figure 8), in agreement with the fact that autoreactivity is more common in the elderly, possibly linked to age-associated B cells[28].

236 In summary, we demonstrated that we could understand the pattern of molecular variation by exploiting the factors, each reflecting distinct types of human biology, behaviour, lifestyle, hormonal
238 use or potential transitions to disease.

CORRELATION NETWORK

240 We performed a correlation analysis, including all the multiomics data as well as an ensemble of quantitative or semi-quantitative measures consisting of clinical data, activity and sleep, fitness test
242 data, and other scores. We computed a cross-correlation network between features of different types using two alternative metrics. For the between-individuals network (BIN), we averaged the
244 measurements from all time points before calculating correlations between features. We also included 146 genetic trait scores obtained by summing up the contribution from all the variants associated with
246 each trait as reported by the GWAS catalog. The within-individuals network (WIN) consisted of linear correlations of repeated measures of pairs of features within-participants. It estimated a common
248 regression slope, representing a measure of association shared among individuals, and resulting from changes occurring at the individual level during the study. The BIN and WIN were calculated after age-

250 and sex-adjustment and p-values were corrected for multiple hypothesis (FDR<0.05). We then identified distinct communities of interconnected features (modules), as an aid for interpretation.

252 Among the strongest correlations of the BIN ($|\rho| > 0.6$), we detected not only pairs measuring the same molecular entity using different assays (i.e. TSH (clinical-PEA), $\rho = 0.96$; Cholesterol (clinical-GCMS)
254 $\rho=0.82$), but also features of different types, for example LDL-receptor protein and triglycerides ($\rho=0.82$) or LEP protein and BMI ($\rho=0.68$). The network consisted of 375 nodes and 570 edges
256 (Supplementary table 5). Several clinical variables represented hubs with the largest number of associated connections to metabolites and proteins (Figure 5). Those hubs were inversely correlated
258 to modifiable behavioural risk factors, consisting in wearable-based measures of physical activity (intense physical activities to insulin, number of steps to waist circumference). Similarly, measures of
260 physical fitness (lower body, abdominal and upper body) inversely correlated with LEP. Notably, the proteins with common genetic defects in familial hypercholesterolemia figured in the cardiometabolic
262 subnetwork, namely LDLR, PCSK9, and apolipoprotein. For instance, PCSK9, a pharmacological target of LDL-lowering therapies, correlated positively to several glycerophospholipids and ApoB, but
264 negatively to CMPF (3-Carboxy-4-methyl-5-propyl-2-furanpropionic acid), a metabolite that is formed from the consumption of fish oil and may have positive metabolic effects[29]. In the whole network, 24
266 GWAS summary scores resulted significantly associated with at least one other node (Supplementary figure 13), and 11 scores concerned haematological measurements (erythrocytes, leucocytes and
268 thrombocytes). While some edges associated the genetic score directly with the corresponding trait measured in this study, especially for haematological traits, other associations occurred between
270 proteins or metabolites and the genetic susceptibility to a disease/trait with cardiometabolic relevance. For example, we observed an inverse association between the score for BMI in physically inactive
272 individuals and several FAEs, carnitine and tyrosine. Furthermore, an inverse association was observed between the score for abdominal aortic aneurysm and IL-6RA levels, supporting the contribution of IL-
274 6 signalling and inflammation to this disease[30]. These observations indicated that the between-individuals variability might be explained at least partly by personal genetic differences.

276 The WIN captured associations between pairs of features that resulted from concordant variation in repeated measures obtained from the same individuals. This source of variation is assumed to be 278 complementary to the BIN, it does not average or aggregate the data, neither does it violate the assumption of independence of the observations. We interpreted the edges in this network as 280 associations resulting from changes occurring over time and not due to baseline between-individuals characteristics. The network consisted of 302 nodes and 611 edges (Supplementary table 5). Only 46 282 edges and 151 nodes were also detected in the BIN, suggesting that a non-overlapping set of correlations were represented. For example, in an inflammation-related subnetwork (Figure 5), hsCRP 284 and leucocytes lay in the proximity of cytokines, cytokine receptors, proteins involved in leukocyte functions and members of the tryptophan metabolic pathway (kyneurine and indoles). This subnetwork 286 was not revealed in the BIN and the observed edges likely originate from individuals transitioning through inflammatory states or infections during the study, although we cannot completely exclude 288 seasonal variation. Other edges specifically observed in the WIN positioned measures of activities and sleep in the proximity of several metabolites and proteins. Among the proteins, we observed well-290 known members of lipid metabolism pathways (LEP, LPL) and proteins with related functions (PTX3[31,32], NRP1[33], PRSS8[34]). Correspondingly, FFA and FAEs appeared in this subnetwork. The above 292 correlations suggested that within-individual dietary factors, changes in fat metabolism and changes in physical activity could be further investigated as motivations for the observed associations. 294 Furthermore, the connection with sleep and physical activity is reminiscent of the link between leptin, circadian rhythm, sleep quality, and obesity[35].

296 PERSONAL TRAJECTORIES

In order to stimulate lifestyle changes and improve health, we defined personalized, actionable 298 possibilities for each participant. This strategy resulted in groupwise significant changes in actionable clinical variables. When considered individual-wise, the changes unfolded into personal trajectories, 300 and often a connection with the multiomics was established. Common behavioural adjustments were related to diet and exercise, illustrated by the case of a 28-year male. The subject underwent positive 302 adaptations resulting in improvement of clinical variables and self-rated health (Figure 2 and Figure 6), in agreement with the nutritional and exercise recommendations. At baseline, he presented with

304 obesity, high systolic blood pressure, dyslipidaemia, elevated insulin levels and elevated hsCRP (Figure 6A). During the study, he reported increases in self-rated health, frequency and amount of
306 exercise (Figure 6C), and these adaptations were confirmed by the activity levels detected by the wearable device (Figure 6B). The sustained level of activity resulted in longitudinal changes in key
308 actionable clinical variables at the end of the study (Figure 6A), including decreased BMI, improved lipid profile, reduced low-grade systemic inflammation, reduced systolic blood pressure, normalization
310 of insulin levels and improvement of the estimated insulin resistance. These interpretable changes reflected variation in the omics domain as well, as shown by the MOFA+ factors (Figure 6D). Indeed,
312 the improvement in the BMI, lipid profile and insulin resistance, combined with an increase in physical activity, is compatible with the observed decrease in F11 values for this subject. We indeed observed
314 longitudinal decrease of obesity- and inflammation-associated proteins and other adaptations suggesting an involvement of the GH/IGF-1 axis. Similarly, the changes in F8 and F10 - associated
316 with fatty acid esters and lipid metabolism - reflected the variation in the total cholesterol levels. Several acylcarnitines peaked at the third visit, suggesting a metabolic adjustment during a transition
318 period toward increased physical activity. For comparison, we show (Figure 2 and Supplementary figure 14) the case of a 36-years female, presenting obesity, dyslipidaemia, hyperinsulinemia and
320 hyperglycaemia at baseline. She was referred to consult her physician and was indeed diagnosed with type 2 diabetes. During the study, phenotypic changes occurred: reduction in the glucose, insulin and
322 cholesterol levels, as a result of therapeutic intervention (Metformin, Atorvastatin, Empagliflozin) and not a genuine lifestyle change with increased physical activity. Correspondingly, the levels of the
324 MOFA+ factors did not change considerably and this individual remained an outlier at all the time points.

326 The case of participant with a respiratory tract infection is illustrated in Supplementary Figure 15, it shows the dysregulation of metabolic pathways during infection as previously observed[1,6], and it
328 highlights the importance of personal metabolic signatures which can be altered during infections.

330 # DISCUSSION

The convergence of systems medicine, digital health, big data, consumer-driven healthcare and social
332 networks is at the heart of the P4 healthcare model. To promote the P4 approach into the current
healthcare systems, longitudinal personalized health intervention studies are needed, and numerous
334 initiatives exist to profile healthy individuals according to the precision medicine principle. However,
fewer studies have simultaneously combined longitudinal multiomics profiling, digital self-tracking and
336 health monitoring, data feedback and tailored lifestyle coaching. We have done all this with a
comprehensive approach and generated a valuable longitudinal data set which can serve both as a
338 resource and a reference for future precision medicine studies. Our study has provided several steps
in the context of precision medicine. Firstly, by adding layers of molecular information and long-term
340 monitoring on top of genomics, we have stressed the importance of including multiomics profiling
other than genomics to precision medicine initiatives. Indeed, current large-scale academic and
342 commercial initiatives largely rely on genetic data connected to health outcomes, while there is a need
for expanding the precision medicine toolbox to include multiomics and functional assays, especially
344 in precision oncology[35,36]. Secondly, by integrating the molecular data with digital health parameters,
we have demonstrated that a connection between the molecular environment and the external
346 manifest characteristics (*phenotype*) occurs and concerns a multiplicity of health and lifestyle aspects,
collected with traditional and emerging modalities, and including adiposity, hormonal influences, diet
348 and physical activity, to mention a few. Our holistic efforts resulted in an unsupervised re-discovery of
known associations between molecular features and indicate that changes in measures from a
350 consumer health wearable device are connected with changes in molecular features. Thirdly, our study
design implemented data feedback and coaching to stimulate lifestyle changes and we anticipate that
352 this model could become broadly applicable to future efforts. However, only information derived from
the genetic data was actively returned to the participants, while the other multiomics data were
354 generated at the end of the study, mostly to minimize systematic biases and batch effects. Currently,
this challenge remains to be solved, especially in the context of precision medicine, where collections
356 can be assembled from n-of-one experiments and longitudinally collected samples, but systematic
biases are common due for example to systematic variations of instrument responses or reagents lots.

358 Our analysis proposed a low-dimensional space to investigate the complexity of the multiomics and the connection to known sources of variation. Among those, sex, age and BMI are among the most
360 studied and often are confounders in association models. For this reason, we regressed out the effect of age and sex in the correlation networks, but we allowed the effect of these covariates to appear in
362 the MOFA+ analysis, in order to verify if separate axes of variability could be retrieved and if they were independent of them. Indeed, we verified that BMI, as a proxy for adiposity and obesity, could only be
364 strongly associated with one factor but it did not influence relevantly the others. Similarly, age and sex associated to a few but not all factors, showing that the identified axes of variation represented a
366 spectrum of molecular variation connected to several lifestyle factors, which cannot simply be explained by the most common predictors mentioned above.

368 One interesting observation is that the use of oral contraceptives containing EE is alone a sufficient element to influence the covariance of the proteome and metabolome, to such extent that one of the
370 identified factors is nearly an indication of the use of this drug. These effects were identified in a data-driven manner and we discovered a distinct dimension of variability in human biology influenced by an
372 external hormone, whose effects are strong enough to be clearly picked up in an unsupervised analysis, above all other causes of variability and noise. F14 could therefore be a potentially useful
374 metric to assess exposure to EE as well as associated health effects. Besides being the major female hormone, estrogen is a fundamental hormone for the maintenance of tissue homeostasis of several
376 tissue types in both males and females, and therefore it is not unexpected that modulation of this pathway has detectable consequences in the proteome and metabolome. However, considering that
378 the exposure to EE from contraceptives could be long-term, what remains to be investigated is either the biological significance of this persistent alteration, but also to what extent this covariate is generally
380 unaccounted in multiomics screens, in view of the fact that similar alterations could be associated to other physiopathological conditions. For example, serum TFF3 was found to be elevated in women
382 with breast cancer[36], and FETUB is a highly abundant liver-secreted protein sensitive to estrogen and increased in type 2 diabetes[37,38].

384 Our analysis showed that part of the variability in the multiomics features could be explained by genetic determinants. This raised the question whether an interaction could exist between the genetic
386 predisposition and the magnitude of the changes observed in clinical and omics variables. We have addressed this subject specifically for the levels of 25(OH)D (vitamin D) and tailored the
388 supplementation guided by genetic markers. The results are presented elsewhere (Sallinen et al., The Journal of Nutrition, in press) and support the evidence that genetic predispositions impact the
390 response to certain lifestyle changes and interventions[39,40].

While the average individual does not exist, empirical evidence and conclusions based on large groups
392 of individuals and summary measures are the norm in experimental research. Under the paradigm of precision medicine and health, this assumption is mitigated by the application of treatment and
394 prevention strategies taking into account the individual variability. However, when highly dense longitudinal multiomics and phenotyping studies are performed, the challenges and drawbacks of
396 aggregating personal profiles are increasing. For example, the presence of outlier measurements for some individuals could be explained by the occurrence of specific events detected by traditional
398 methods or inferred from the use of wearable devices. Indeed, the use of wearable devices offer the opportunity of continuously monitoring the participants, therefore allowing the detection of acute
400 events or behaviours that would be missing when registering outcomes with traditional methods or when averaging across time. Our data contribute to the accumulating evidence that personal
402 multiomics signatures show individual dynamics and associate with specific physiological or pathological events[1,6,7].

404 We have to acknowledge limitations of our study. Firstly, the small sample size limits the discovery of novel associations and implies that the conclusion should be confirmed in larger cohorts to have
406 further empirical evidence. Nevertheless, we retrieved several known associations, likely resulting from strong underlying effect sizes. For example, we showed that several blood cell measures in our study
408 are under genetic control, in agreement with the high heritability of hematological traits[41]. By extension, it is possible that the associations with cardiometabolic relevance observed in our study have also
410 larger true effect sizes. While this is a limitation for the discovery of unknown relationships, it is on the

contrary important from the translational point of view, because our study qualifies as a resource for extracting further candidate investigations, especially in medically relevant terms.

Because of the highly personalized, non-structured nature of the coaching, our work does not strictly qualify as an interventional study, and we have to recognize the lack of a proper control group not receiving data feedback and coaching. A certain heterogeneity in the individual adherence to the recommendations might bias the conclusions based on aggregated measures. We have shown that individual trajectories and multiomics profiles exists and our data collection can propose certain connections only when specific cases were considered. For example, in the case of activity and sleep tracking, we observed good overall engagement, although the compliance over time was not constant for all the individuals. In addition, a certain seasonality cannot be excluded and indeed periodicity in immune systems gene expression and cellular composition is often investigated[42,43]. Therefore, seasonality might have a contribution in influencing the changes occurring at the within-individual level.

Our study is truly a forerunner in shaping person centric data driven care for the future. It demonstrated not only the power of combination of multi-omics data and lifestyle data, but new opportunities for the healthcare system to design their services towards predictive data-driven care and support individuals in lifestyle changes. New data sets, like multiomics measurements and continuous monitoring via wearable devices will shape the traditional disease-based healthcare. However, more research is needed to truly enhance the proactive, personalized health maintenance for the benefit of individuals, and society.

METHODS

ETHICAL PERMIT AND CONSENT

The study was conducted in line with the Declaration of Helsinki and approved by the Coordinating Ethics Committee of the Helsinki University Hospital, Finland. Each participant provided informed written consent for the study and the biobanking of samples and data. Participants were free to drop out any time, but their samples and data were still available for analyses. If a participant withdrew the consent, samples and data were discarded.

OVERVIEW

The study was conducted at the Institute for Molecular Medicine Finland (FIMM), HiLIFE, University of Helsinki, Finland, between September 2015 and January 2017. Recruitment was performed in September 2015, and five study visits followed, approximately every four months, (Supplementary Figure 1). Every visit included a health check-up and blood and urine sampling. Before or after every visit, participants collected fecal and saliva samples, filled out a questionnaire, and performed fitness tests. Data on physical activity and sleep was collected from the second visit onward with an activity watch. Key actionable health data were returned to the participants via a web dashboard starting at the second visit. Tailored health and wellness advice and coaching was provided by two personal trainers from the third visit onward. Between visits 4 and 5, participants could compare their data to summary measures calculated with the other participants' data.

ELIGIBILITY CRITERIA AND RECRUITMENT

The requirements included: age of 25-64 years at the study start, sufficient computer skills and Internet access via a smartphone compatible with the provided smartwatch; sufficient English language knowledge to be able to understand simple messages and to use health and wellness applications. We excluded individuals with severe diseases (cancer, cardiovascular, debilitating neurological, psychiatric or orthopaedic diseases). However, individuals with risk factors for chronic diseases (e.g.,

obesity, elevated blood pressure, dyslipidaemias, disturbances in sugar metabolism, mild forms of
456 metabolic syndrome, smoking, moderate drinking or sleep problems) were allowed. Individuals diagnosed with or suspected of having rare monogenic diseases were excluded. In addition,
458 individuals under custody, with special needs or with limited decisional capacity were excluded, as well as people suffering from severe forms of alcoholism and depression. Pregnant women were
460 excluded and women becoming pregnant during the study were no longer asked to provide samples or contribute to the study. Altogether, 645 clients of a private occupational health service (Mehiläinen
462 Töölö, Helsinki, Finland) were invited to participate (Supplementary Figure 1). People interested in participating (n=125) filled out a questionnaire to assess eligibility. A total of 107 volunteers of
464 European descent from the Helsinki metropolitan area were selected to participate and 96 completed the study (Supplementary Table 1).

466 *RETURN OF PERSONAL HEALTH DATA*

The ensemble of anthropometrics, clinical laboratory tests, and physiological measurements is called
468 clinical variables in this paper. We returned actionable health data via the Health Dashboard web application, which allowed participants to: explore and compare their data against reference values
470 and the mean values for the other participants, fill out questionnaires and read informational material. The clinical variables and their reference values were returned starting at visit 2. A physician interpreted
472 the clinical data and was available to discuss the results with the participants. The occupational health service communicated any medically-relevant finding requiring immediate actions, while the study
474 group communicated non-acute findings. Clinical decisions were made according to the national Current Care Guidelines (https://www.kaypahoito.fi/). Genetic data were returned to participants under
476 the guidance of a clinical geneticist after visit 2. A personal 10-year risk for coronary heart disease (CHD) was communicated using KardioKompassi[44]. The risk model is based on both traditional (sex,
478 age, family history, smoking, systolic blood pressure, total and HDL cholesterol) and hereditary risk factors (approximately 49,000 SNPs). If the risk was >10% the participant was referred to a doctor.
480 We also communicated the risk for low serum 25(OH)D concentration after visit 4 (Sallinen et al., The Journal of Nutrition, in press). We returned visualizations of questionnaire data on diet, physical

482 activity, sitting, sleeping, subjective health status, and mental wellbeing after visit 4. We also determined a self-reported obstructive sleep apnea risk score[45]. Participants were able to monitor their
484 physical activity and sleep data using the Withings Health Mate app starting at visit 2.

Coaching and group meetings

486 Two personal trainers (PTs) coached participants from visit 3 onward. Coaching included nine 30-minute private meetings (three face-to-face and six remote), email/phone support, as well as group
488 meetings. The PTs were accredited by the European Health and Fitness Association. No structured, evidence-based coaching protocol was used, but personal actionable possibilities were defined to
490 help participants change their behaviour and improve their health. With the help of a physician and a nutritionist, the PTs translated and customized actionable possibilities to specific recommendations.
492 The PTs had access to participants' age, clinical variables, fitness test data, and information about their occupation, exercise, and diet. Tailored health advice and coaching were based on each
494 participant's behaviour, health risks, lifestyle, and goals. One to three relevant, personalized and actionable opportunities were offered to guide and motivate participants to make lifestyle changes to
496 optimize wellness and health and delay predicted pathologies. Personalized advice usually focused on diet, exercise, mental wellbeing, or stress and time management. If necessary, a physician limited
498 exercise. Twenty-one informational group meetings were organized during the study, where participants could interact with a physician, a nutritionist, a nurse, PTs, and other experts. Participation
500 in these meetings was voluntary except for the first, during which a physician and a geneticist interpreted the clinical variables data as well as the CHD risk prediction.

502 Experimental procedures

Health check-up and clinical variables

504 Health check-ups occurred on weekdays between 7:30 and noon. Body weight, height, waist and hip circumferences, blood pressure, and pulse were measured using standard procedures. Participants
506 were asked about medications, dietary supplements, and the use of health care services. Blood and

urine samples were collected at every visit. Fasting (≥8 h) blood samples were collected, and clinical chemistry assays were performed on blood, plasma or serum, at the diagnostic laboratory of Mehiläinen Töölö (Helsinki, Finland), United Medix Laboratories Ltd (Helsinki, Finland) and HUS Diagnostic Center (Helsinki, Finland). Urine samples (≥2 h without urinating) were collected using standard procedures. A dipstick test was performed on the urine samples at the diagnostic laboratory of Mehiläinen Töölö (Helsinki, Finland). Aliquots of blood, plasma, serum and urine were frozen at -20°C and stored in liquid nitrogen for biobanking.

Questionnaire

Before every visit, participants filled out an online questionnaire, including approximately 150-190 questions, depending on the visit, and covering the following: personal information; sociodemographic and socioeconomic characteristics; familial and individual disease history; functional capacity and health; mental wellbeing; physical activity and exercise habits; diet (including food frequency questionnaire, FFQ); smoking; alcohol consumption; sleep; occupational health; personality traits; attitudes and expectations towards lifestyle changes; monitoring own health and wellbeing; expectations towards health technology. Healthy Food Intake Index is a food-based diet quality index, calculated from the FFQ data and adapting an available method[46].

Fitness tests

After every visit, participants were instructed to perform lower-body (squats, repetitions/30s), abdominal (sit-ups, repetitions/30s) and upper-body (push-ups, max number of repetitions) muscular fitness, balance and mobility tests. Participants executed the tests and uploaded the results to the Health Dashboard.

Activity and sleep monitoring

After the second visit, participants were equipped with the Withings Activité Pop smartwatch, connected to the Withings Health Mate app, to measure physical activity, energy expenditure and sleep. Participants were requested to wear the watch until the end of the study. Wellness Warehouse

532 Engine [47] embedded in the Health Dashboard was used to authorize and provide the research group access to participants' data. Only aggregated daily activity and sleep data were exported and included
534 in this study.

SALIVARY CORTISOL

536 Participants collected saliva samples within two weeks of every visit, using Cortisol-Salivette® with a synthetic swab (Sarstedt). Four samples (awakening, 15 min and 30 min after wake up, bedtime) were
538 collected on a typical weekday. Time and mood at sampling were recorded. Samples were stored at +4°C until aliquoting and storage at -20°C. Salivary cortisol levels were determined at the University
540 of Trier (Trier, Germany) using a DELFIA immunoassay [48]. The stress scores derived from the measurements inlcuded: AUCi, AUCg (according to[49]), awakening, evening, peak and Delta (peak -
542 ground) cortisol levels.

DNA EXTRACTION AND GENOTYPING

544 DNA was extracted from whole blood with Chemagic MSM1 (PerkinElmer). Genotyping was performed at the FIMM Technology Centre (HiLIFE, University of Helsinki, Finland) using InfiniumCoreExome-24
546 v1.0 DNA Analysis Kit, iScan system and standard reagent and protocols (Illumina). Genotypes were pre-phased with ShapeIT2 and imputed with IMPUTE2. Two pre-phased reference panels were used
548 (--merge_ref_panels): 1000G Phase 1 and a Finnish low-coverage WGS imputation reference panel, composed of 1,941 whole-genome sequences (SISu project). Imputation resulted in 30.3 million
550 quality-filtered variants (R^2>0.3 and missingness<0.05).

GCMS AND LCMS

552 GCMS and LCMS experiments were performed at the Swedish Metabolomics Center (Umeå). 100 µl of plasma were processed as described[50], with the following details: extraction with 900 µl of 90% v/v
554 methanol, containing internal standards for both GCMS and LCMS, at 30 Hz for 2 minutes; protein precipitation at +4 °C; centrifugation at +4 °C, 14 000 rpm, 10 minutes. 50 or 200 µl of supernatant
556 were evaporated to dryness in a speed-vac concentrator, for GCMS or LCMS analysis respectively,

and stored at -80 °C. Quality control (QC) samples were created by pooling supernatants. MSMS
558 analysis (LCMS) was run on the QC samples for identification purposes. Sample batches were created
according to a randomized run order. For GCMS, derivatization and analysis were performed as
560 described previously[50], with the following modifications: 0.5 µL of derivatized sample; splitless injection
with a L-PAL3 autosampler (CTC Analytics AG); 7890B gas chromatograph (Agilent Technologies);
562 chemically bonded 0.18 µm Rxi-5 Sil MS stationary phase (Restek Corporation); column temperature
increased from 70 to to 320 °C at 40 °C/min; Pegasus BT TOFMS (Leco Corporation); solvent delay of
564 150 s; detector voltage 1800-2300 V. Unprocessed MS-files were exported from the ChromaTOF
software in NetCDF format to MATLAB R2016a (Mathworks), where processing occurred, including
566 baseline correction, chromatogram alignment, data compression and Multivariate Curve Resolution.
The extracted mass spectra were identified by comparisons of their retention index and mass spectra
568 with known libraries using the NIST MS 2.0 software[51]. Annotation was based on reverse and forward
searches in the library. LCMS experiments were performed as described[52] and all data processing was
570 performed using the Masshunter Profinder version B.08.00 (Agilent Technologies). The processing was
performed both in a target and an untargeted fashion. For target processing, a predefined list of
572 metabolites commonly found in plasma and serum were searched for using the Batch Targeted feature
extraction in Masshunter Profinder. An-in-house LCMS library, built up by authentic standards run on
574 the same system with the same chromatographic and MS settings, was used for the targeted
processing. The identification of the metabolites was based on MS, MSMS and retention time
576 information.

AUTOANTIBODY BEAD ARRAYS

578 Autoantibody profiling on antigen bead arrays was performed as previously described[27], at the
Autoimmunity and Serology Profiling facility at SciLifeLab (Stockholm).

580 *PEA*

Plasma proteins were quantified using Proximity Extension Assay (PEA) at Olink Bioscience (Uppsala),
582 using 6 panels: Cardiometabolic, CVD II, CVD III, Inflammation I, Metabolism and Oncology II. Each

panel assayed 92 proteins using a matched pair of antibodies coupled to oligonucleotides, which form
584 an amplicon by proximity extension and can be quantified by real-time PCR. The data were normalized
against an extension control and an interplate control and expressed as Normalized Protein
586 eXpression (NPX) values, which represent an arbitrary relative quantification unit on log2 scale. The
NPX values below the limit of detection (LOD) were considered missing and their value was replaced
588 with the LOD value for each assay.

MICROBIOME ANALYSIS

590 Participants collected faecal samples within two weeks of every visit. Samples were collected in
precooled vials placed in styrofoam boxes with ice gel packs and then stored at +4°C for a maximum
592 of one day until aliquoting, freezing at -20°C, and storage in liquid nitrogen without additives. Thawed
faecal samples were spun-down and DNA was extracted, with 50 ng of DNA submitted to PCR
594 amplification as described[53], using 341f and 805r primers (CCTACGGGNGGCWGCAG and
GTGBCAGCMGCCGCGGTAA) for the V3–V4 regions of 16S rRNA[54]. Sequencing was done on an
596 Illumina MiSeq with 2x250 bp reads. After quality trimming with Cutadapt, an ASV (amplified sequence
variants) table was generated using the DADA2 pipeline[55], including the following steps: filtering and
598 trimming, learning of error rates, dereplication, sample inference, read pairs merging, removal of
chimeras and taxonomy assignment using SILVA v128 database.

600 BIOINFORMATIC ANALYSES

LONGITUDINAL ANALYSIS

602 We applied Generalized Estimating Equations (GEE) to the quantitative clinical variables to investigate
the longitudinal changes while controlling for sex and age. As data feedback and coaching started
604 respectively from visit two and three, we excluded the first visit and considered the second visit as
baseline. Four time points (0-4) were then considered and we aimed at extracting the average change
606 per visit, assuming the same change in the values between any two successive visits. Furthermore,
for each variable, individuals were classified as Out-Of-Range at Baseline (OORB) if the values were

outside the reference range (Supplementary Table 2) at baseline. We assumed that the longitudinal changes could be distinct for individuals classified as ORRB. In other words, we allowed the effect of coaching and data feedback to be different in the two groups by introducing an interaction term. If the OORB group included at least five individuals, then the variable was modelled as:

value ~ Sex + Age + Time.point + OORB + Time.point:OORB

Otherwise, a model with no groups of individuals was considered:

value ~ Sex + Age + Time.point

GEE models were fitted using the geepack library and exchangeable correlation structure. We extracted the effects, their standard errors and p-values using the `esticon` function in the doBy library. If no interaction was specified, the coefficient for Time.point represented the estimated change for all the individuals, expressed as the change occurring between two successive visits. If the interaction was included, we considered the change occurring in the ORRB group between two successive visits, and we extracted the effect as the linear combination of the coefficients of Time.point and OORB. P-values were adjusted with the Benjamini-Hochberg method. Model prediction of the variable values was visualized by stratifying for sex and OORB group. The 95% confidence levels were estimated by bootstrapping with 1000 replications.

DIMENSIONALITY REDUCTION

We selected the quantitative clinical variables and imputed missing using the `imputePCA` function in the missMDA package. Principal Component Analysis (PCA) was performed with the `PCA` function in the FactoMineR package on scaled data. Variable contribution to a given PC was defined as the ratio between the squared cosine of a variable and the sum of the squared cosines for all the variables for that component.

DATA PREPROCESSING

Activity and sleep. We obtained summary measures for the activity and sleep data by calculating average values for the different variables in the previous 30 days before each visit. We considered only samples for which at least 10 days were included in the calculation.

GCMS. The relative quantities (RQs) were log2-transformed and missing values were imputed with the KNN algorithm. Data were normalized using the RUV4 method in the ruv R library [56]. `RUV4` was applied to remove sources of technical variability, including batch effect and the signal drift over time. Briefly, we used the internal standards (IS) as negative controls, k=4 and a design matrix with individuals and visits as covariates, in order to estimate the matrix W of unwanted factors and their respective α coefficients. The number of factors to remove (k) was chosen with the `getK` routine, but was ensured not to exceed 1/3 of the number of the IS. The normalized relative concentrations were obtained by subtracting the effect of the W components from the RQs. The IS values were inspected before and after normalization to ensure a removal of the signal drift over time and a reduction of the Coefficient of Variation (CV). Estimation of the Intraclass Correlation Coefficient (ICC) and PCA plots were also evaluated to inspect the performance of the normalization method.

LCMS. The negative and positive modes from LCMS experiments were processed separately. Unidentified metabolite peaks and metabolites with more than 25% of missing data were removed. RQs were log2-transformed and missing values were imputed with KNN. `RUV4` adjustment and inspection of the results were performed as described above with k=2 or k=1 for LCMS-neg and LCMS-pos data, respectively.

Autoantibodies. We considered: continuous Median Fluorescence Intensity (MFI), discrete binned and binary (0=undetected, 1=detected) data (see [27]). MFI values were normalized with the Probabilistic Quotient Normalization[57], with a median reference profile, and then log2-transformed.

16S rRNAseq. The ASV count table represents an analog of the traditional Operational Taxonomic Unit table. We inspected the taxa prevalence (the number of samples in which a taxon has nonzero counts) and the total abundance (sum of the counts in all samples) and the abundance distribution. Using phyloseq, we agglomerated the counts to the genus level, to reduce functional redundancy. The

genus-level data were filtered to remove taxa with missing phylum annotation, prevalence ≤2 and total
658 abundance ≤10. We inspected the ordination of the samples using several distance metrics. We then converted the genus-level count to a DESeq2 dataset and used the Variance Stabilizing
660 Transformation (VST), which normalizes with respect to the library size and gives a matrix of approximately homoscedastic values that can be used for downstream analyses. As a major source
662 of batch effect was represented by the experimental plate, we verified that the VST conversion also reduced the library size effect by visualizing the sample ordination, using MDS with Bray-Curtis
664 distance for the genus-level counts and Euclidean distance for the VST values. We also formally tested the reduction of the batch effect, by looking at the association between the first two axes of the sample
666 ordination plots with the plate ID. The estimation of the α-diversity for each sample was done using the original unfiltered counts.

668 *INTEGRATION OF MULTIOMICS EXPERIMENTS*

A MultiAssayExperiment object was assembled with all the continuous clinical and omics data, namely
670 RUV4-nomalized data for GCMS, LCMS-neg and LCMS-pos, log2MFI for autoantibodies, NPX values for PEA assays and VST-transformed values for 16S counts. Data filtering to remove unwanted
672 features included: removal of internal standards from GCMS and LCMS; removal of proteins NPX values < LOD (i.e. missing data) in more than 25% of the samples; removal of FS, CCL22 and BDNF
674 (technical issues, Olink communication); removal of autoantibodies with background fluorescence in all samples (scored reactivity values ≤0.5); removal of bacterial taxa with a prevalence ≤30%. We used
676 the filtered object for all the downstream analyses. The resulting dataset included 136 GCMS metabolites, 104 LCMS-neg metabolites, 163 LCMS-pos metabolites, 174 autoantibodies, 501
678 proteins and 85 bacterial taxa (Supplementary table 2).

VARIANCE PARTITION ANALYSIS

680 For each omics type, between- and within-individual variation was inspected with a distance-based method and with variance partitioning analysis. For the distance method, Euclidean distance between
682 all pairs of samples was calculated. Then, the within-individual distance was calculated as the median

value of the distance values of the sample pairs from the same individual. This value was plotted together with the distribution of the remaining distance values, i.e. the distances between one individual and the rest of the individuals. For the variance partitioning method, a linear mixed model was fitted with lme4 R library, independently to each feature with nonzero variance. We included the individual as a random intercept and age, sex and time point (0-4) as fixed effects. The fixed effect variance, random intercept variance and residual variance components were extracted and the relative fraction calculated. The random intercept variance represented the between-individual variance, while we interpreted the residual variance as the within-individual variance not accounted by the fixed effects.

Multi-Omics Factor Analysis

Multi-Omics Factor Analysis v2 (MOFA+) provides a set of factors that capture biological and technical sources of variability[11,12]. It infers the axes of heterogeneity that are shared across multiple modalities and those specific to individual data modalities. We used the "intercept_factor" branch of the code repository (https://github.com/bioFAM/MOFA2/tree/intercept_factor). For training, we selected the samples that had a measurement in all the omics layers (n=359). We considered a Gaussian likelihood for the continuous measurements for all the layers, except for autoantibodies, which were considered in their binary form (0=undetected, 1=detected) with Bernoulli likelihood. Data were not scaled. We trained 10 alternative models in Python with a random seed, starting from 20 factors and the following options: iter="10000", convergence_mode="medium", dropR2="0.02". The model with the best value of the Evidence Lower Bound (ELBO) was selected. We checked the robustness of the learned factors by inspecting the Pearson correlation between the factors obtained by all the runs (Supplementary Figure 6). We then computed the fraction of the total variance explained by each factor and the fraction of variance explained by each factor in each layer. We inspected the factor loadings to understand the contribution of the original features. A feature with a higher absolute loading has a higher weight on the factor, but because the loadings are not directly comparable, their scaled values were used for visualization. The sign of the loading defines a direct (positive) or inverse (negative) proportionality with

the corresponding factor, and features with similar loadings contribute similarly to the factor. We
710 inspected the factor values and to visualize and cluster the samples on the reduced space.

ASSOCIATION BETWEEN FACTORS AND PHENOTYPIC VARIABLES

712 In order to test the association between the MOFA+ factors and the sample characteristics, we gathered a collection of phenotypic information including: clinical variables; questionnaire data (family
714 history, exercise and physical activity, functional capacity and health, mental health, diet, smoking, alcohol use and sleep habits); Healthy Food Intake Index; KardioKompassi risk; sleep apnea score;
716 stress scores; fitness tests; sleep and activity summaries from the wearables. For each combination of factor and phenotypic variables, we fitted a linear model with the factor values as outcome and the
718 phenotypic variable as predictor. Reported R^2 values were derived from these models. For the categorical variables, the predictor was considered an ordered factor if the factor levels corresponded
720 to ordered levels and the variable could be considered as a qualitative or semi-quantitative ordinal variable. A False Discovery Rate (FDR) was calculated using the Benjamini-Hochberg method. The
722 candidate associations for further screening were obtained at FDR<0.05, while the associations reported in Figure 3 satisfy a FDR<0.001 threshold, in order to better control for false positives arising
724 from the multiple hypotheses tested. The selected associations were refined with linear mixed models as implemented in lme4 library. We modelled the LF values with the individual as a random intercept
726 and age and sex as fixed effect. We refer to these models as the covariate-adjusted models. P-values for these models were obtained with the "Type II ANOVA" as implemented in the `Anova` function in
728 the car library, with a Kenward-Roger F test.

POPULATION STRATIFICATION

730 The DHR and the 1000 Genome phase 3 genotypes were merged. Analyses were done with PLINK v1.9. Only autosomal biallelic SNPs with genotyping rate >95% and MAF>5%. were considered. A set
732 SNPs in approximate Linkage Disequilibrium was obtained with the option --indep-pairwise 50 5 0.2 and PCA was performed. To predict the ethnicity, a Linear Discriminant Analysis model (`lda` in MASS)
734 was trained in R with the PCA scores of the 1000 Genomes only and tested on the DHR samples.

GWAS SUMMARY SCORES

We considered 146 traits from the GWAS catalog v1.0.1 (https://www.ebi.ac.uk/gwas/) for selected ontology categories: body measurement, cardiovascular disease, cardiovascular measurement, hematological measurement, inflammatory measurement, lipid or lipoprotein measurement, liver enzyme measurement, metabolic disorder and other (fasting blood glucose, vitamin D levels and thyroid stimulating hormone). For each trait, only the studies meeting the following criteria were considered: at least one SNP with p-value<1E-08, sample size >5000, at least 10 SNPs reported. The study with the largest sample size was considered for the traits with multiple associated studies. For each biallelic SNPs, the reported effect size of the risk allele was considered as a weight. Summary scores were computed by multiplying the imputed genotype dosage of each risk allele times its respective weight and summing across all SNPs.

BETWEEN- AND WITHIN-INDIVIDUAL CROSS CORRELATION NETWORK

We considered the continuous measurements for all the omics layers, together with a collection of measurements including: GWAS summary scores; gut microbiome alpha diversity; clinical variables; questionnaire data; Healthy Food Intake Index; KardioKompassi risk; sleep apnea score; stress scores; fitness tests; sleep and activity summaries. The resulting dataset was preprocessed by regressing out the effect of sex and then the effect of age for each variable, only if significantly associated. For the between-individual cross correlation network calculation, the observations were grouped by individual and averaged, obtaining 96 independent observations for each of the 1394 variables. Spearman correlation was calculated for each pair of variables, resulting in 731318 nonmissing estimated ρ coefficients, p-values and Benjamini-Hochberg adjusted p-values (FDR), for the pairs of features of different types (activity and sleep, autoantibody, clinical variables, fitness test, genetic, HFII, KardioKompassi, metabolite, microbial, protein, sleep apnea score, stress score). For the within-individual cross-correlation network calculation, the GWAS scores and the autoantibody data were excluded, resulting in 1058 variables, 96 individuals and 5 time points. We used rmcorr library [58] to estimate the common within-individual association for grouped values measured at the five visits. `rmcorr` estimates a common regression slope representing the association shared among individuals

762 and provides the best linear fit for each individual using parallel regression lines with different intercepts. The repeated-measures correlation coefficient (r_{rm}) is similar to the Pearson correlation
764 coefficient and measures the strength of a linear association but, unlike Pearson correlation, it takes into account non-independence between the measures. Hence, we estimated 347640 nonmissing r_{rm},
766 p-values and Benjamini-Hochberg adjusted p-values (FDR), for the pairs of features of different types and with at least 100 nonmissing pairs of values. For downstream analysis, we selected the
768 associations satisfying the condition FDR<0.05 and coefficient>0.3 (ρ or r_{rm}), and generated two annotated correlation networks. Communities were extracted with the Louvain method, resulting in
770 modularity values of 0.70 and 0.69 for the between- and within-individuals correlation network respectively.

772

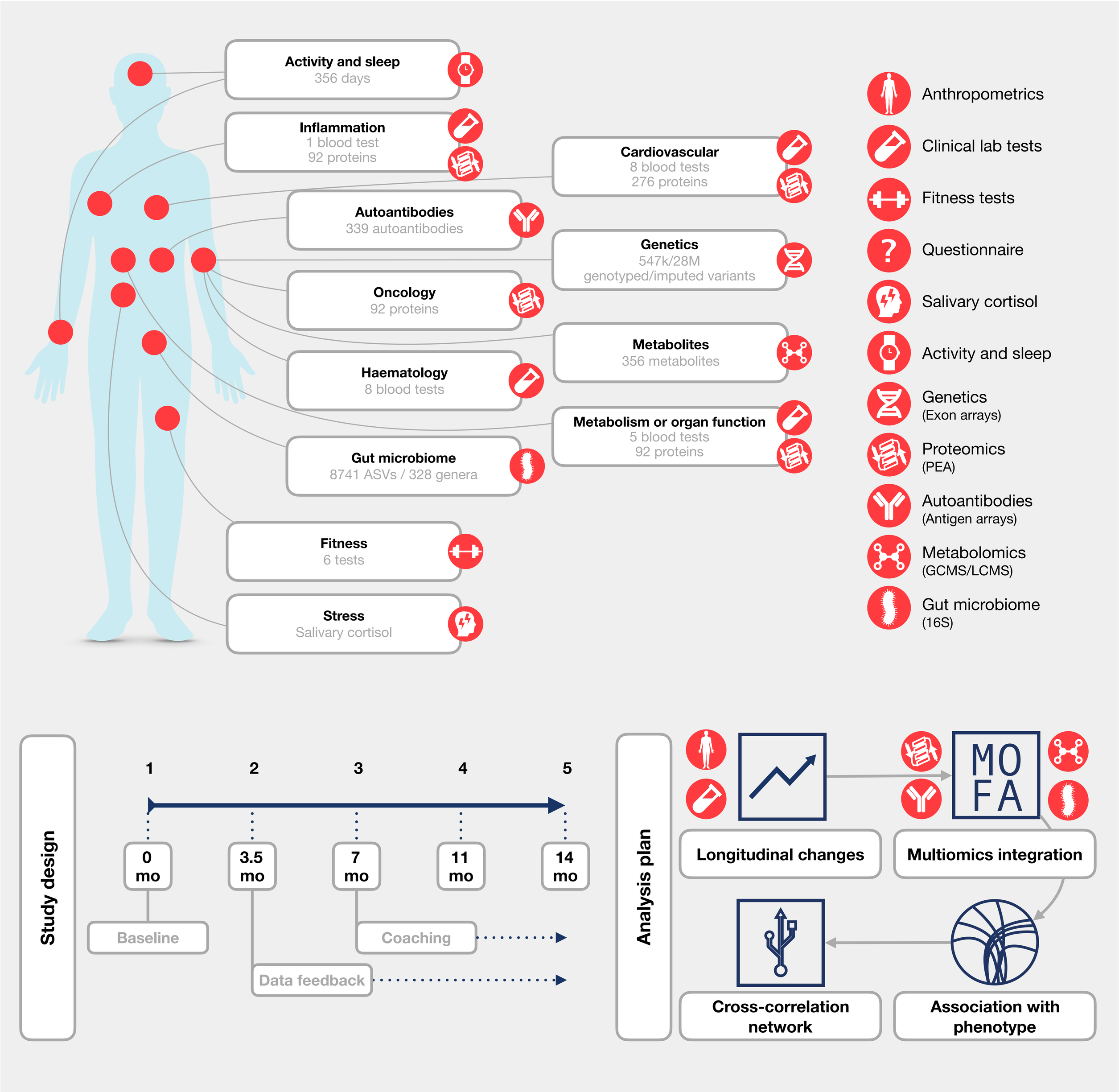

Figure 2: Overview of the measured features, longitudinal design and analysis workflow.

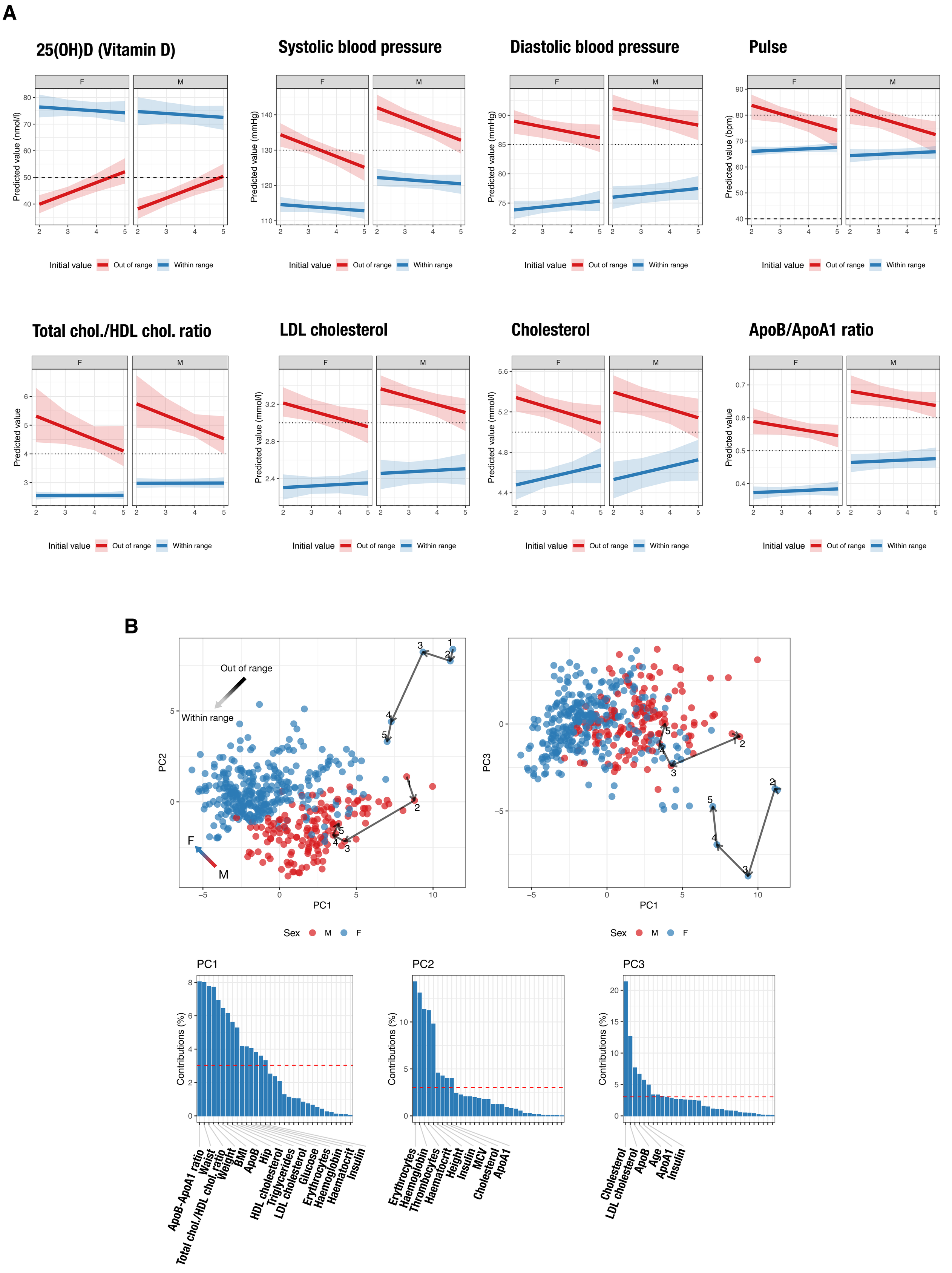
A
25(OH)D (Vitamin D)
Systolic blood pressure
Diastolic blood pressure
Pulse
Total chol./HDL chol. ratio
LDL cholesterol
Cholesterol
ApoB/ApoA1 ratio
F
M
Predicted value (nmol/l)
Predicted value (mmHg)
Predicted value (bpm)
Predicted value
Predicted value (mmol/l)
Initial value
Out of range
Within range
B
Out of range
Within range
PC1
PC2
PC3
Sex
M
F
Contributions (%)
ApoB-ApoA1 ratio
Waist
Total chol./HDL chol. ratio
Weight
BMI
ApoB
Hip
HDL cholesterol
Triglycerides
LDL cholesterol
Glucose
Erythrocytes
Haemoglobin
Haematocrit
Insulin
Erythrocytes
Haemoglobin
Thrombocytes
Haematocrit
Height
Insulin
MCV
Cholesterol
ApoA1
Cholesterol
LDL cholesterol
ApoB
Age
ApoA1
Insulin

Figure 2: A. Longitudinal analysis reveals the positive effect of data feedback and coaching on health. Generalized Estimating Equation (GEE) model prediction for the significantly changed variables (FDR<0.05), stratified by sex and out/within range status at baseline. For this analysis, the second visit represented a baseline because data feedback and coaching started at the 2nd and 3rd visits respectively (blue: within range, red: out of range). Bootstrapped confidence intervals are shown. **B.** Principal components plot of the individuals obtained using all the numerical clinical variables. The trajectories for two selected individuals along successive study visits are shown with arrows. The loadings for the first three PCs are shown in the bottom panels and the variables with relative contribution higher than average (red line) are named.

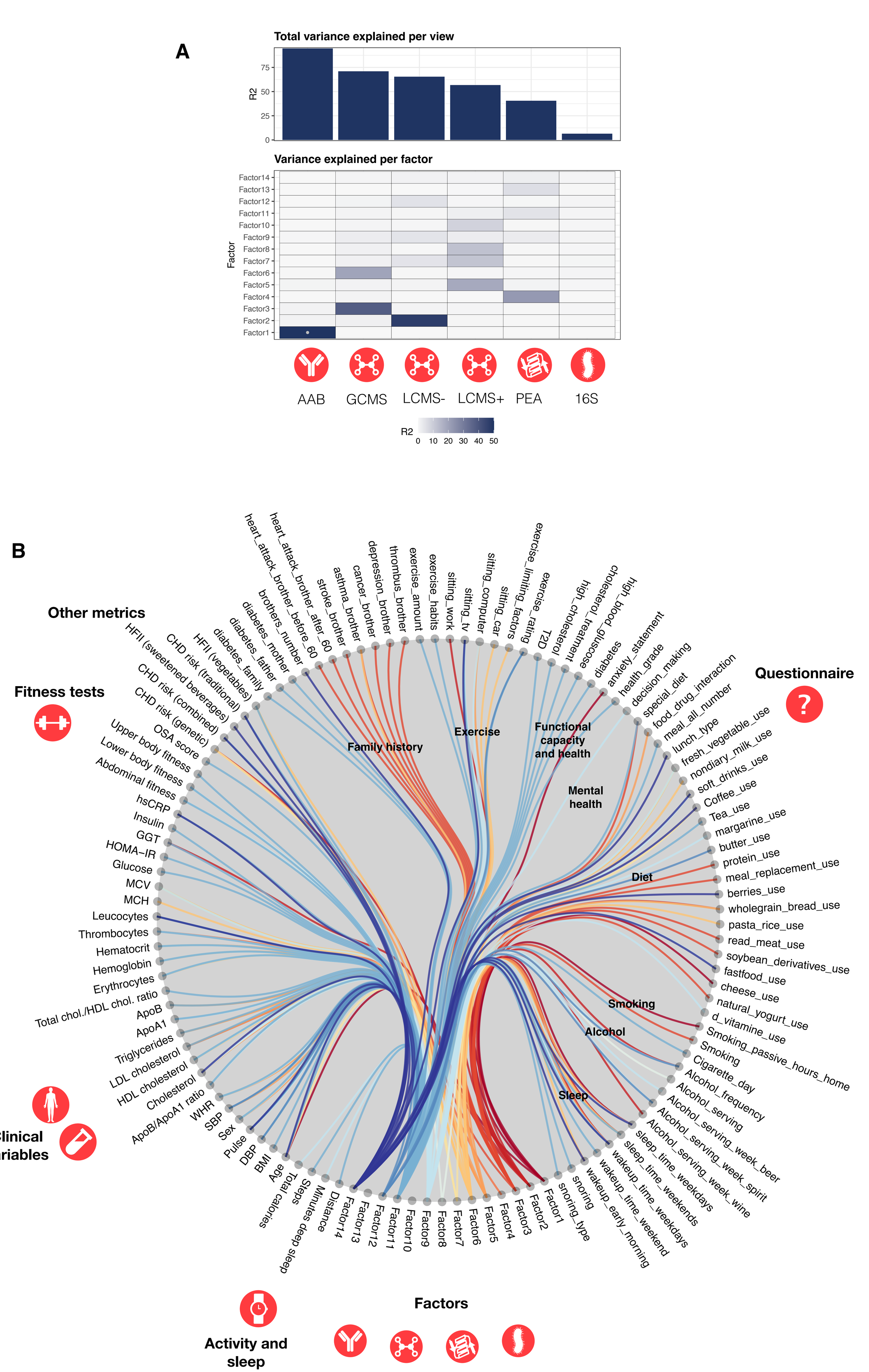
A
Total variance explained per view
R2
75
50
25
0
Variance explained per factor
Factor
Factor14
Factor13
Factor12
Factor11
Factor10
Factor9
Factor8
Factor7
Factor6
Factor5
Factor4
Factor3
Factor2
Factor1
AAB
GCMS
LCMS-
LCMS+
PEA
16S
R2
0 10 20 30 40 50
B
Other metrics
Fitness tests
Clinical variables
Activity and sleep
Factors
Questionnaire
Family history
Exercise
Functional capacity and health
Mental health
Diet
Smoking
Alcohol
Sleep
HFII (sweetened beverages)
CHD risk (traditional)
CHD risk (combined)
CHD risk (genetic)
HFII (vegetables)
OSA score
diabetes_family
Upper body fitness
diabetes_father
Lower body fitness
diabetes_mother
Abdominal fitness
diabetes_number
hsCRP
brothers_number
Insulin
heart_attack_brother_after_60
GGT
heart_attack_brother_before_60
HOMA–IR
stroke_brother
Glucose
asthma_brother
MCV
cancer_brother
MCH
depression_brother
Leucocytes
thrombus_brother
Thrombocytes
exercise_amount
Hematocrit
exercise_habits
Hemoglobin
sitting_work
Erythrocytes
sitting_tv
Total chol./HDL chol. ratio
sitting_computer
ApoB
sitting_car
ApoA1
exercise_limiting_factors
Triglycerides
exercise_rating
LDL cholesterol
T2D
HDL cholesterol
high_cholesterol_treatment
Cholesterol
high_blood_glucose
ApoB/ApoA1 ratio
diabetes
WHR
anxiety_statement
SBP
health_grade
Sex
decision_making
Pulse
special_diet
DBP
food_drug_interaction
BMI
meal_all_number
Age
lunch_type
Total calories
fresh_vegetable_use
Steps
nondiary_milk_use
Minutes deep sleep
soft_drinks_use
Distance
Coffee_use
Factor14
Tea_use
Factor13
margarine_use
Factor12
butter_use
Factor11
protein_use
Factor10
meal_replacement_use
Factor9
berries_use
Factor8
wholegrain_bread_use
Factor7
pasta_rice_use
Factor6
read_meat_use
Factor5
soybean_derivatives_use
Factor4
fastfood_use
Factor3
cheese_use
Factor2
natural_yogurt_use
Factor1
d_vitamine_use
snoring_type
Smoking_passive_hours_home
snoring
Smoking
wakeup_early_morning
Cigarette_day
wakeup_time_weekend
Alcohol_frequency
wakeup_time_weekdays
Alcohol_serving
sleep_time_weekends
Alcohol_serving_week_beer
sleep_time_weekdays
Alcohol_serving_week_spirit
Alcohol_serving_week_wine

Figure 3. A. Variance decomposition. Percentage of total variance explained (R^2) for each data layer (up) or variance explained (R^2) for each factor and data layer (bottom). A dot marks the out-of-bound value (>50%) for autoantibodies. **B.** Association with phenotype. The factor values were tested for their association with the phenotypic variables and the top associations (FDR<0.001) are shown. The edges are bundled according to their category and colored based on the originating factor.

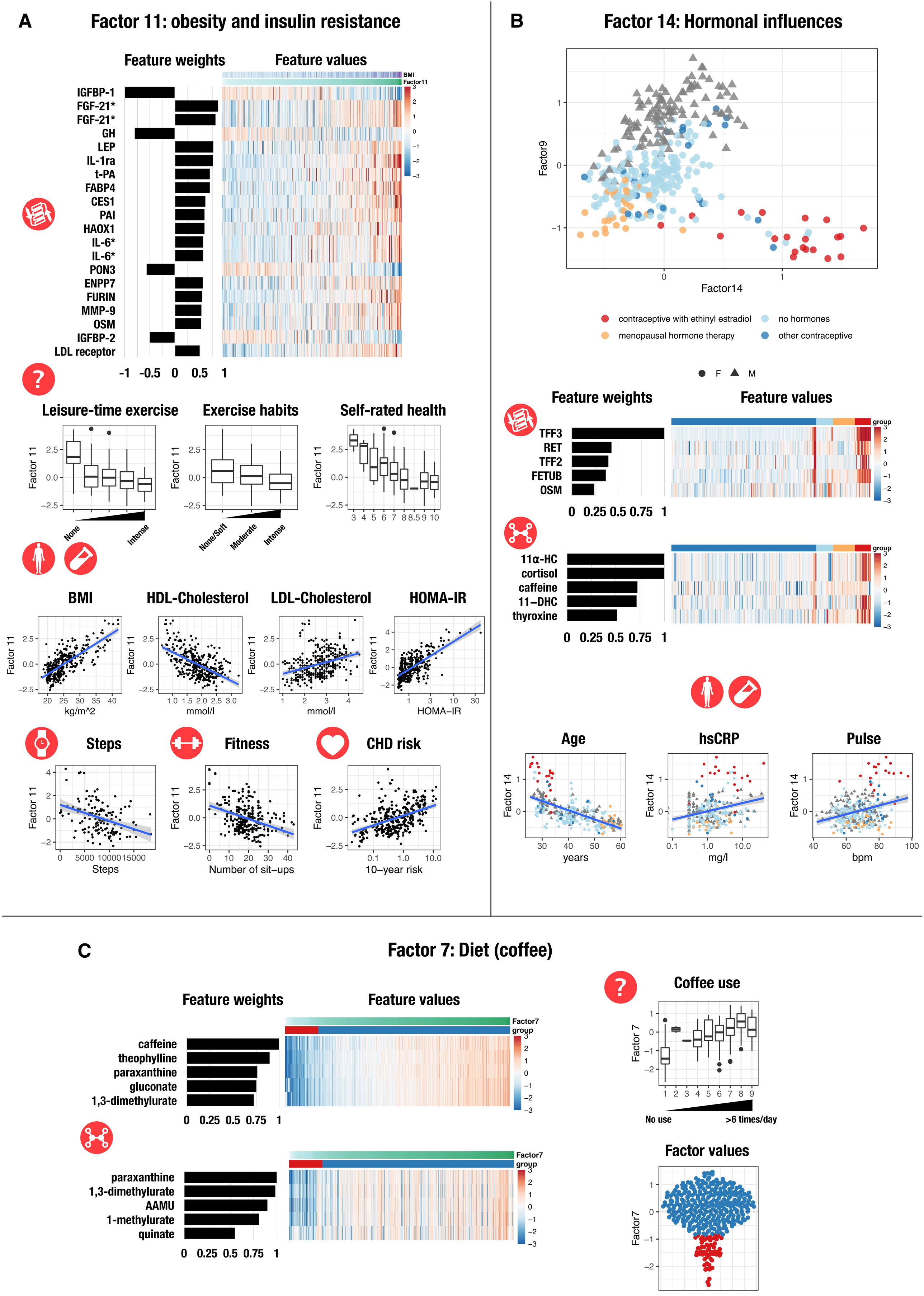
A
Factor 11: obesity and insulin resistance
Feature weights
Feature values
BMI
Factor11
IGFBP-1
FGF-21*
FGF-21*
GH
LEP
IL-1ra
t-PA
FABP4
CES1
PAI
HAOX1
IL-6*
IL-6*
PON3
ENPP7
FURIN
MMP-9
OSM
IGFBP-2
LDL receptor
-1 -0.5 0 0.5 1
Leisure-time exercise
None
Intense
Exercise habits
None/Soft
Moderate
Intense
Self-rated health
BMI
kg/m^2
HDL-Cholesterol
mmol/l
LDL-Cholesterol
mmol/l
HOMA-IR
Steps
Steps
Fitness
Number of sit–ups
CHD risk
10–year risk
Factor 11
B
Factor 14: Hormonal influences
Factor9
Factor14
contraceptive with ethinyl estradiol
no hormones
menopausal hormone therapy
other contraceptive
F
M
Feature weights
Feature values
group
TFF3
RET
TFF2
FETUB
OSM
0 0.25 0.5 0.75 1
11α-HC
cortisol
caffeine
11–DHC
thyroxine
Age
years
hsCRP
mg/l
Pulse
bpm
Factor 14
C
Factor 7: Diet (coffee)
Feature weights
Feature values
Factor7
group
caffeine
theophylline
paraxanthine
gluconate
1,3-dimethylurate
0 0.25 0.5 0.75 1
paraxanthine
1,3-dimethylurate
AAMU
1-methylurate
quinate
Coffee use
Factor 7
No use
>6 times/day
Factor values
Factor7

Figure 4. A. Factor11 is linked to obesity and insulin sensitivity. The top scaled protein weights for Factor11 are shown as well as their values (row z-score). The association between the factor values for each sample and the phenotypic variables is shown. A regression line with 95% confidence interval is shown when appropriate. An asterisk marks the proteins measured on multiple PEA panels. **B.** Factor14 is influenced by hormones. A scatterplot of Factor9 and Factor14 values shows that samples can be separated based on the sex (Factor9) and the use of hormones (Factor14). Factor14 identifies a group of young women using contraceptives with ethinyl estradiol (red). The top metabolites and proteins with positive scaled weights on Factor14 are shown. The original feature values are shown as a heatmap (row z-score). The association between the factor values for each sample and the phenotypic variables is shown, as well as a regression line with 95% confidence interval. Points are coloured as in the top panel. Abbreviations: 11α-HC: 11alpha–hydrocortisone, 11–DHC: 11–dehydrocorticosterone. **C.** Factor7 is associated to coffee consumption. The scaled positive weights are shown for the top metabolites, as well as their values. The association between the factor values with self-reported coffee consumption is shown. A two-group classification of the samples based on Factor7 values was obtained with gaussian-mixture modeling and shown with colored dots (red: lower coffee consumption, blue: higher coffee consumption).

A Between-individuals

Cardiometabolic

PAPPA
AR
PAI
FABP4
SEZ6L
Distance
Gal-9
Steps
hsCRP
NPTXR
CLMP
KYAT1
Hip
1-arachidoyl-GPC (20...
1-docosapentaenoyl-G...
Total calories
Waist
PAF (18:0)
Cysteine, S-methyl-,...
Pulse
Weight
TYROSINE
BMI
OSA score
IGFBP-1
Lachnospiraceae_Copr...
SERINE
Upper body fitness
t-PA
RTN4R
IL1RL2
Intense activities
ALCAM
PON3
Abdominal fitness
MERTK
FETUB
IL-1ra
CITRIC ACID
LEP
IGFBP-2
2-palmitoyl-GPE* (16...
OSM
RARRES2
PRSS8
FURIN
CES1
LDL-receptor
1-pentadecanoylglyce...
Lower body fitness
alpha-CEHC
CHI3L1
CTSD
CDHR5
PAF(12:0)
CD164
1-palmitoylplasmenyl...
LOX-1
ApoA1
1-stearoylplasmenyle...
Insulin
SERPINA7
thyroxine
HDL cholesterol
1-myristoyl-GPC (14:...
CPE
NOMO1
Total chol./HDL chol...
Hypoxanthine
PAF (14:1)
ERBB3
TRAIL
MMP-9
Leucocytes
Triglycerides
palmitoleoyl-GPC* (1...
PLTP
ApoB/ApoA1 ratio
1-eicosatrienoyl-GPC...
APOM
CCL16
TRAIL
gamma-glutamylalanin...
ApoB
F7
Notch-3
1-eicosapentaenoylgl...
TNFSF14
SERPINA5
Hydroxyoctadecenoyl-...
2-arachidonoyl-GPE* ...
PLA2G7
SCGB3A2
PCSK9
uPA
MMP-2
LILRA5
gamma-glutamylleucin...
PROC
BMP-6
CHD risk (combined)
PTPRS
uPA
Cholesterol
CHOLESTEROL
CFHR5
aspartylleucine
Hydroxyisovaleroylca...
TR-AP
FCN2
3-Carboxy-4-methyl-5...
alpha-Tocopherol
Hydroxylauroyl-carni...
LDL cholesterol
Beta-alanine
1-linoleoyl-GPE (18:...
Protein C levels
LAMP2_aAb
Lipoprotein phosphol...
TWEAK
TFPI
LDL cholesterol
SOX10_aAb

B Within-individuals

Activity and sleep

GLYCEROL-3-PHOSPHATE
Cholesta-3,5-diene
Minutes in bed
SOST
Defluviitaleaceae_De...
Laurylcarnitine (C12...
2-Hydroxyoctanoate
Weight
Octanoyl-carnitine (...
Glutarylcarnitine (C...
Minutes deep sleep
1-myristoyl-GPC (14:...
Minutes awake
3-Hydroxydecanoate
Calories
beta-D-Glucopyranose
Carnitine
Moderate activities
PAF(12:0)
LEP
cis-4-decenoyl carni...
Dodecenoyl-carnitine...
Rhodospirillaceae_NA
Steps
leucylglycine
Eicosadieneoyl-carni...
PRSS8
Hydroxyisovaleroylca...
Soft activities
3-HYDROXYBUTYRIC ACI...
Decanoylcarnitine (C...
NRP1
Tetradecadienyl-carn...
BMI
Minutes light sleep
1-nonadecanoylglycer...
Distance
Myristoleoylcarnitin...
SCGB3A2
Oleoylcarnitine (C18...
Intense activities
Acetylcarnitine (C2:...
Hexadecenoyl-carniti...
THBS4
IDUA
PTX3
Uracil
Myristoylcarnitine (...
citrulline
LPL
Butyrylcarnitine (C4...
THREONINE
OCTADECENOIC ACID,-9...
TLT-2
5-acetylamino-6-amin...
Hydroxyoctadecenoyl-...
Hydroxymyristoyl-car...
Hydroxylauroyl-carni...
(R*,S*)-2,3-Dihydrox...

Inflammation

TNF-R2
TNFSF13B
CD160
IL-12B
GZMB
kynurenine
XCL1
IL-18BP
5-hydroxyindoleaceta...
IL-10
CXCL9
2-oxindole-3-acetate
CCL3
CEACAM8
ITGAV
OSM
HGF
CCL24
CDCP1
CXCL10
IL2-RA
TNFRSF6B
IL-6
SERPINA5
Gal-9
CXCL11
Malic acid
HGF
IL-6
hsCRP
MIP-1-alpha
Citric acid
FABP4
Hypoxanthine
Leucocytes
PRTN3
HDL cholesterol
IL-1ra
CCL4
PGLYRP1
CTSV
CPE
NADK
MPO
MCP-2
COMP
Protein-BOC
IL27
CSF-1
LOX-1
MMP-9
VEGF-A
CYR61
MMP-10
Pulse
riboflavin (Vitamin ...

Data type (node color)

- Proteins
- Metabolites
- Biometrics
- Genetic scores
- Autoantibodies
- Activities and sleep
- Gut microbiome
- Other

Correlation (edge color)

- +

Figure 5. Cross-correlation network analysis aids the interpretation the relationship between data types. Only associations between features of different type were considered to calculate correlation networks at FDR<0.05. The size of the nodes is proportional to the node degree and the edge thickness is proportional to the magnitude of the correlation. The node color indicate different data types. The proteins appearing twice in the network were measured on multiple PEA panels. **A.** Selected between-individual subnetwork. **B**. Selected within-individual network modules.

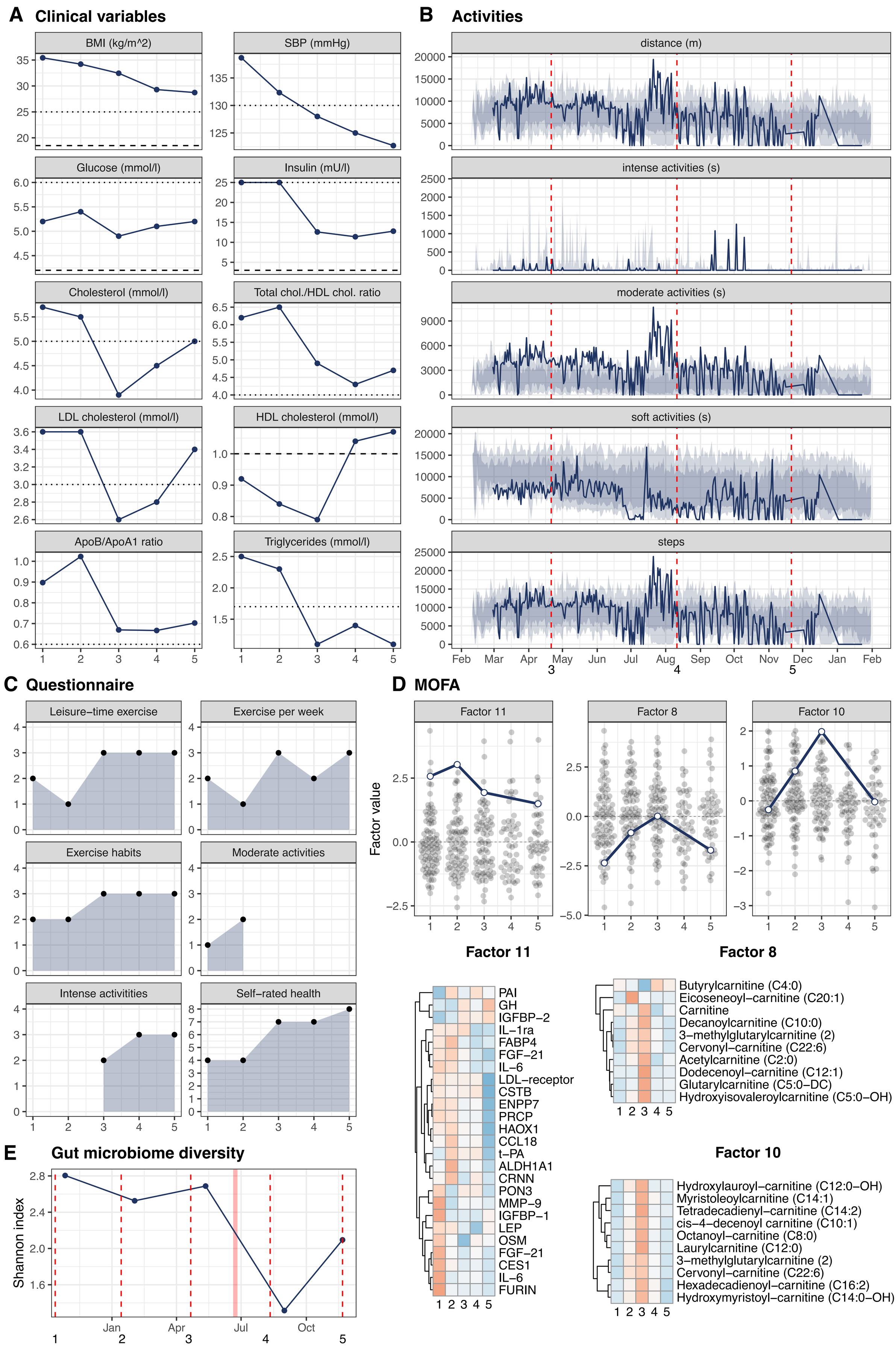
A Clinical variables
BMI (kg/m^2)
SBP (mmHg)
Glucose (mmol/l)
Insulin (mU/l)
Cholesterol (mmol/l)
Total chol./HDL chol. ratio
LDL cholesterol (mmol/l)
HDL cholesterol (mmol/l)
ApoB/ApoA1 ratio
Triglycerides (mmol/l)
B Activities
distance (m)
intense activities (s)
moderate activities (s)
soft activities (s)
steps
Feb Mar Apr May Jun Jul Aug Sep Oct Nov Dec Jan Feb
C Questionnaire
Leisure−time exercise
Exercise per week
Exercise habits
Moderate activities
Intense activitities
Self−rated health
D MOFA
Factor 11
Factor 8
Factor 10
Factor value
PAI
GH
IGFBP−2
IL−1ra
FABP4
FGF−21
IL−6
LDL−receptor
CSTB
ENPP7
PRCP
HAOX1
CCL18
t−PA
ALDH1A1
CRNN
PON3
MMP−9
IGFBP−1
LEP
OSM
FGF−21
CES1
IL−6
FURIN
Butyrylcarnitine (C4:0)
Eicoseneoyl−carnitine (C20:1)
Carnitine
Decanoylcarnitine (C10:0)
3−methylglutarylcarnitine (2)
Cervonyl−carnitine (C22:6)
Acetylcarnitine (C2:0)
Dodecenoyl−carnitine (C12:1)
Glutarylcarnitine (C5:0−DC)
Hydroxyisovaleroylcarnitine (C5:0−OH)
Hydroxylauroyl−carnitine (C12:0−OH)
Myristoleoylcarnitine (C14:1)
Tetradecadienyl−carnitine (C14:2)
cis−4−decenoyl carnitine (C10:1)
Octanoyl−carnitine (C8:0)
Laurylcarnitine (C12:0)
3−methylglutarylcarnitine (2)
Cervonyl−carnitine (C22:6)
Hexadecadienoyl−carnitine (C16:2)
Hydroxymyristoyl−carnitine (C14:0−OH)
E Gut microbiome diversity
Shannon index
Jan Apr Jul Oct

Figure 6. A case study: lifestyle change in one individual and the associated molecular changes. **A.** Clinical variables showing longitudinal changes. Reference values are shown (dashed line: lower normal value, dotted line: upper normal value) **B.** Daily summary of the activities recorder by the smart watch included: distance, time spent in intense, moderate or soft activities and number of steps. The shaded area correspond to the 10, 25, 75 and 90 percentiles in the whole population. The study visits are marked with vertical dashed lines **C.** Selected lifestyle questions. The numbers correspond to orderer categories, where a higher number corresponds to higher frequency or more favorable outcome. **D.** Longitudinal values for selected MOFA+ factors (blue line) plotted together with the factor values for the remaining samples at each study visit (grey dots). **E.** Gut microbiome diversity (Shannon index). The vertical dashed line mark the date for the study visit, which could be different than the fecal sample collection date (dots). A red shaded area mark a period of antibiotic treatment.

774

Supplementary Table 1

	Unit	Value at baseline (n=96)
Age	years (mean ± SE)	40.9 ± 0.9
Sex	counts (M/F)	30/66
BMI	kg/m^2 (mean ± SE)	24.9 ± 0.5
Alcohol consumption	g/week (mean ± SE)	53.1 ± 5.4
Current smokers[1]	%	16[2]
Education >12 years	%	87
Physical exercise ≥ 3 times/week	%	56
Married or cohabiting	%	67
Hypercholesterolemia (Cholesterol> 5 mmol/l)	%	44
Hypertriglyceridemia (Females: 20-30y, >1.5; 30-50y, >1.7; >50y, >2 Males: 20-30y, >1.7; >30y, >2)	%	4
Overweight or obesity (BMI>25 kg/m^2)	%	38
Elevated blood pressure (SBP > 130 mmHg)	%	31
Low vitamin D (25(OH)D<50 nmol/l)	%	31
Hyperglycemia (Fasting glucose>6 nmol/l)	%	8
Anemia (Hb<117 (F) or Hb<134 (M) g/l)	%	2
Self-reported obstructive sleep apnea	%	2

776

778

[1] Participants who reported regular smoking were defined as current smokers.

[2] n=94

Supplementary table 2. List of all the included features and their annotation.

780 (see separate Excel file)

782 **Supplementary table 3. Results from the GEE model**

	Estimate	Units	CI	P-value	FDR	Type	# of OORB
Hip circumference	-0.667	cm	-0.957 – -0.377	6.34E-06	8.87E-05	All	1
25(OH)D	4.072	nmol/l	2.336 – 5.808	4.29E-06	8.87E-05	OORB	24
Systolic blood pressure	-3.078	mmHg	-4.469 – -1.688	1.43E-05	1.33E-04	OORB	27
Diastolic blood pressure	-0.947	mmHg	-1.443 – -0.451	1.81E-04	1.01E-03	OORB	22
Pulse	-3.214	bpm	-4.876 – -1.551	1.52E-04	1.01E-03	OORB	9
Total/HDL cholesterol ratio	-0.405		-0.66 – -0.150	1.88E-03	8.77E-03	OORB	7
LDL cholesterol	-0.085	mmol/l	-0.139 – -0.030	2.21E-03	8.83E-03	OORB	29
ApoB/ApoA1 ratio	-0.014		-0.024 – -0.005	3.89E-03	1.36E-02	OORB	35
Cholesterol	-0.084	mmol/l	-0.145 – -0.024	5.83E-03	1.81E-02	OORB	36

784 **Supplementary table 4. Associations between MOFA factor values and phenotypic variables.**

786 (see separate Excel file)

Supplementary table 5. Edge lists for the Between- and Within-Individual Networks.

(see separate Excel file)

REFERENCES

1. Chen, R. *et al.* Personal omics profiling reveals dynamic molecular and medical phenotypes. *Cell* **148,** 1293–1307 (2012).
2. Chen, R. *et al.* Longitudinal personal DNA methylome dynamics in a human with a chronic condition. *Nat Med* **6,** 1 (2018).
3. Perkins, B. A. *et al.* Precision medicine screening using whole-genome sequencing and advanced imaging to identify disease risk in adults. *Proc Natl Acad Sci USA* **115,** 3686–3691 (2018).
4. Piening, B. D. *et al.* Integrative Personal Omics Profiles during Periods of Weight Gain and Loss. *Cell Systems* **6,** 157–170.e8 (2018).
5. Price, N. D. *et al.* A wellness study of 108 individuals using personal, dense, dynamic data clouds. *Nat Biotechnol* **35,** 747–756 (2017).
6. Zhou, W. *et al.* Longitudinal multi-omics of host-microbe dynamics in prediabetes. *Nature* **569,** 663–671 (2019).
7. Schüssler-Fiorenza Rose, S. M. *et al.* A longitudinal big data approach for precision health. *Nat Med* **25,** 792–804 (2019).
8. Ahadi, S. *et al.* Personal aging markers and ageotypes revealed by deep longitudinal profiling. *Nat Med* **26,** 83–90 (2020).
9. Tebani, A. *et al.* Integration of molecular profiles in a longitudinal wellness profiling cohort. *Nat Commun* **11,** 1–14 (2020).
10. Digital Health Revolution. *digitalhealthrevolution.fi* Available at: http://www.digitalhealthrevolution.fi/uploads/2/4/1/5/24155377/person_centric_data_management_models_and_opportunities_in_health_care_sector_full.pdf. (Accessed: 22nd October 2020)
11. Argelaguet, R. *et al.* Multi-Omics Factor Analysis—a framework for unsupervised integration of multi-omics data sets. *Mol Syst Biol* **14,** e8124 (2018).
12. Argelaguet, R. *et al.* MOFA+: a probabilistic framework for comprehensive integration of structured single-cell data. *biorxiv* **18,** 837104 (2019).
13. Considine, R. V. *et al.* Serum immunoreactive-leptin concentrations in normal-weight and obese humans. *N Engl J Med* **334,** 292–295 (1996).
14. Juge-Aubry, C. E. *et al.* Adipose tissue is a major source of interleukin-1 receptor antagonist: upregulation in obesity and inflammation. *Diabetes* **52,** 1104–1110 (2003).
15. Zheng, Z. *et al.* Interacting hepatic PAI-1/tPA gene regulatory pathways influence impaired fibrinolysis severity in obesity. *J. Clin. Invest.* **130,** 4348–4359 (2020).
16. Xu, A. *et al.* Adipocyte fatty acid-binding protein is a plasma biomarker closely associated with obesity and metabolic syndrome. *Clinical Chemistry* **52,** 405–413 (2006).
17. Fisher, F. M. *et al.* Obesity is a fibroblast growth factor 21 (FGF21)-resistant state. *Diabetes* **59,** 2781–2789 (2010).
18. Mayne, J. *et al.* Associations Between Soluble LDLR and Lipoproteins in a White Cohort and the Effect of PCSK9 Loss-of-Function. *J. Clin. Endocrinol. Metab.* **103,** 3486–3495 (2018).
19. Kopchick, J. J., Berryman, D. E., Puri, V., Lee, K. Y. & Jorgensen, J. O. L. The effects of growth hormone on adipose tissue: old observations, new mechanisms. *Nat Rev Endocrinol* (2019). doi:10.1038/s41574-019-0280-9
20. Shih, D. M. *et al.* PON3 knockout mice are susceptible to obesity, gallstone formation, and atherosclerosis. *FASEB J.* **29,** 1185–1197 (2015).
21. Nam, S. Y. *et al.* Effect of obesity on total and free insulin-like growth factor (IGF)-1, and their relationship to IGF-binding protein (BP)-1, IGFBP-2, IGFBP-3, insulin, and growth hormone. *Int J Obes* **21,** 355–359 (1997).
22. Meulenberg, P. M. M., Ross, H. A., Swinkels, L. M. J. W. & Benraad, T. J. The effect of oral contraceptives on plasma-free and salivary cortisol and cortisone. *Clinica Chimica Acta* **165,** 379–385 (1987).

23. Barsivala, V., Virkar, K. & Kulkarni, R. D. Thyroid functions of women taking oral contraceptives. *Contraception* **9,** 305–314 (1974).
24. Hodson, L., Skeaff, C. M. & Fielding, B. A. Fatty acid composition of adipose tissue and blood in humans and its use as a biomarker of dietary intake. *Progress in Lipid Research* **47,** 348–380 (2008).
25. Ussher, J. R., Elmariah, S., Gerszten, R. E. & Dyck, J. R. B. The Emerging Role of Metabolomics in the Diagnosis and Prognosis of Cardiovascular Disease. *J. Am. Coll. Cardiol.* **68,** 2850–2870 (2016).
26. Egan, B. M., Greene, E. L. & Goodfriend, T. L. Nonesterified fatty acids in blood pressure control and cardiovascular complications. *Curr. Hypertens. Rep.* **3,** 107–116 (2001).
27. Neiman, M. *et al.* Individual and stable autoantibody repertoires in healthy individuals. *Autoimmunity* **52,** 1–11 (2019).
28. Rubtsova, K., Rubtsov, A. V., Cancro, M. P. & Marrack, P. Age-Associated B Cells: A T-bet-Dependent Effector with Roles in Protective and Pathogenic Immunity. *J Immunol* **195,** 1933–1937 (2015).
29. Prentice, K. J. *et al.* CMPF, a Metabolite Formed Upon Prescription Omega-3-Acid Ethyl Ester Supplementation, Prevents and Reverses Steatosis. *EBioMedicine* **27,** 200–213 (2018).
30. Paige, E. *et al.* Interleukin-6 Receptor Signaling and Abdominal Aortic Aneurysm Growth Rates. *Circ Genom Precis Med* **12,** e002413 (2019).
31. Ristagno, G. *et al.* Pentraxin 3 in Cardiovascular Disease. *Front Immunol* **10,** 1357 (2019).
32. Bonacina, F. *et al.* Pentraxin 3 deficiency protects from the metabolic inflammation associated to diet-induced obesity. *Cardiovasc Res* **115,** 1861–1872 (2019).
33. Wilson, A. M. *et al.* Neuropilin-1 expression in adipose tissue macrophages protects against obesity and metabolic syndrome. *Sci Immunol* **3,** (2018).
34. Frateschi, S. *et al.* PAR2 absence completely rescues inflammation and ichthyosis caused by altered CAP1/Prss8 expression in mouse skin. *Nat Commun* **2,** 161 (2011).
35. Pan, W. & Kastin, A. J. Leptin: a biomarker for sleep disorders? *Sleep Med Rev* **18,** 283–290 (2014).
36. Ishibashi, Y. *et al.* Serum TFF1 and TFF3 but not TFF2 are higher in women with breast cancer than in women without breast cancer. *Sci. Rep.* **7,** 4846 (2017).
37. Floehr, J. *et al.* Association of high fetuin-B concentrations in serum with fertilization rate in IVF: a cross-sectional pilot study. *Hum. Reprod.* **31,** 630–637 (2016).
38. Meex, R. C. *et al.* Fetuin B Is a Secreted Hepatocyte Factor Linking Steatosis to Impaired Glucose Metabolism. *Cell Metab* **22,** 1078–1089 (2015).
39. Zubair, N. *et al.* Genetic Predisposition Impacts Clinical Changes in a Lifestyle Coaching Program. *Sci. Rep.* **9,** 6805 (2019).
40. Walker, C. G. *et al.* Genetic predisposition to an adverse lipid profile limits the improvement in total cholesterol in response to weight loss. *Obesity (Silver Spring)* **21,** 2589–2595 (2013).
41. Okada, Y. & Kamatani, Y. Common genetic factors for hematological traits in humans. *J. Hum. Genet.* **57,** 161–169 (2012).
42. Dopico, X. C. *et al.* Widespread seasonal gene expression reveals annual differences in human immunity and physiology. *Nat Commun* **6,** 7000 (2015).
43. Lakshmikanth, T. *et al.* Human immune system variation during one year. *biorxiv* **17,** 2020.01.22.915025 (2020).
44. Widén, E. & Ripatti, S. Assessment of multifactorial coronary artery disease by utilizing genomic data. *Duodecim* **133,** 776–781 (2017).
45. Niiranen, T. J., Kronholm, E., Rissanen, H., Partinen, M. & Jula, A. M. Self-reported obstructive sleep apnea, simple snoring, and various markers of sleep-disordered breathing as predictors of cardiovascular risk. *Sleep Breath* **20,** 589–596 (2016).
46. Meinilä, J. *et al.* Healthy Food Intake Index (HFII) - Validity and reproducibility in a gestational-diabetes-risk population. - PubMed - NCBI. *BMC Public Health* **16,** 3 (2016).

47. Honko, H. *et al.* W2E--Wellness Warehouse Engine for Semantic Interoperability of Consumer Health Data. *IEEE J Biomed Health Inform* **20,** 1632–1639 (2016).
48. Dressendörfer, R. A., Kirschbaum, C., Rohde, W., Stahl, F. & Strasburger, C. J. Synthesis of a cortisol-biotin conjugate and evaluation as a tracer in an immunoassay for salivary cortisol measurement. *J. Steroid Biochem. Mol. Biol.* **43,** 683–692 (1992).
49. Pruessner, J. C., Kirschbaum, C., Meinlschmid, G.2003. Two formulas for computation of the area under the curve represent measures of total hormone concentration versus time-dependent change. *Elsevier* doi:10.1016/S0306-4530(02)00108-7
50. A, J. *et al.* Extraction and GC/MS analysis of the human blood plasma metabolome. *Anal. Chem.* **77,** 8086–8094 (2005).
51. Schauer, N. *et al.* GC-MS libraries for the rapid identification of metabolites in complex biological samples. *FEBS Lett* **579,** 1332–1337 (2005).
52. Diamanti, K. *et al.* Intra- and inter-individual metabolic profiling highlights carnitine and lysophosphatidylcholine pathways as key molecular defects in type 2 diabetes. *Sci. Rep.* **9,** 1–13 (2019).
53. Hugerth, L. W. *et al.* No distinct microbiome signature of irritable bowel syndrome found in a Swedish random population. *Gut* **69,** 1076–1084 (2020).
54. Hugerth, L. W. *et al.* DegePrime, a program for degenerate primer design for broad-taxonomic-range PCR in microbial ecology studies. *Appl Environ Microbiol* **80,** 5116–5123 (2014).
55. Callahan, B. J. *et al.* DADA2: High-resolution sample inference from Illumina amplicon data. *Nat Meth* **13,** 581–583 (2016).
56. Gagnon-Bartsch, J. A., Jacob, L., Univ, T. S. T. R. F. D. S.2013. Removing unwanted variation from high dimensional data with negative controls.
57. Dieterle, F., Ross, A., Schlotterbeck, G. & Senn, H. Probabilistic quotient normalization as robust method to account for dilution of complex biological mixtures. Application in 1H NMR metabonomics. *Anal. Chem.* **78,** 4281–4290 (2006).
58. Bakdash, J. Z. & Marusich, L. R. Repeated Measures Correlation. *Front Psychol* **8,** 456 (2017).